Technical Support for the Long-Term Deployment of an L-Band Radiometer at Concordia Station

Yearly Report – Data Acquisition and Processing Report
Fourth Year – D3- D6
March 2017

EUROPEAN SPACE AGENCY STUDY
ESTEC Contract 4000105872/12/NL/NF

Prepared by

Giovanni MACELLONI, Marco BROGIONI, Francesco Montomoli
IFAC- CNR, Florence, ITALY

DATE: 30/5/2017
Version: 1.0
Deliverable of the contract: D6-D3

Consiglio Nazionale delle Ricerche
Istituto di **F**isica **A**pplicata "Nello **C**arrara"
VIA MADONNA DEL PIANO N. 10 - CAP 50019 SESTO FIORENTINO FIRENZE

This page is intentionally left blank

ESA STUDY CONTRACT REPORT

ESTEC CONTRACT NO:	SUBJECT:		CONTRACTOR:
4000105872/12/NL/NF	Technical Support for the Long-Term Deployment of an L-Band Radiometer at Concordia Station		IFAC
ESA CR ( )NO:	STAR CODE:	No of volumes: 1 This is volume no: 1	CONTRACTOR'S REF: Deliverable

ABSTRACT:

The work described in this report was done under ESA Contract. Responsibility for the contents resides in the authors or organisation that prepared it.

PREPARED BY:

GIOVANNI MACELLONI, MARCO BROGIONI, FRANCESCO MONTOMOLI -IFAC

ESA STUDY MANAGER:	ESA BUDGET HEADING:
TANIA CASAL	

DOCUMENT CHANGE LOG

Issue/ Revision	Date	Observations
1/0	May 2017	First issue –Draft Version

ABBREVIATIONS

AEP	Annual Executive Project
AWS	Automatic Weather Station
CVA-ARABBA	Avalanche Center of Arabba, Italy
ESA	European Space Agency
IASH	International Association of Scientific Hydrology
IFAC-CNR	Institute of Applied Physics – National Research Council
INGV	Istituto Nazionale di Geofisica e Vulcanologia
IOP	Intensive Operational Period
MZS	Mario Zucchelli Station
NOP	Normal Operational Period
OMT	OrthoMode Transducer
PNRA	Programma Nazionale RIcerche in Antartide
RFI	Radio Frequency Interference
RR	Readiness Review Document – D1 of the contractTEC Total Electron Content

This page is intentionally left blank.

TABLE OF CONTENTS

1 Purpose and structure of document

Purpose

This document contains the Fourth Year Report for DOMEX-3 experiment, prepared by the Institute for Applied Physics "Nello Carrara" – Firenze within the framework of the ESA contract N. 4000105872/12/NL/NF.

In the document is described the execution of the activity carried out in the fourth experimental year of the project (i.e. from January 2016 to January 2017). It includes the description of the fourth summer campaign 2016-2017 as well as the activity conducted during fourth year of the winter campaign and in Italy.

The document is divided into sections in which the individual points were discussed.

2 Overview

The Domex-3 experiment is the follow on of two previous experiments called Domex-1 and Domex-2 which were successfully conducted at Concordia base, Antarctica, by IFAC-CNR in cooperation to ESA (contracts N. 18060/04/NL/CB [1] and N. 22046/08/NL/EL, 20066/06/NL/EL [2]) and PNRA.

The results obtained in these contracts demonstrated that DOME- C represents a unique “high”-temperature (i.e. higher than 150 K), extended target that provides a temporally-stable reference which potentially meets existing requirements for assessing the long-term stability of space-borne L-band radiometric instruments.

In order to meet this objective, co-located ground measurements are required in order to verify target stability over time and to monitor changes in target characteristics that may affect the long-term reference signal: for example, surface roughness or “crusting”, which in spite of being quite stable, appears to evolve with time (possibly due to climatic changes) and may affect the brightness temperature. Long-term monitoring of DOME-C is also crucial to investigating further and to modeling variations in H-pol observed during the DOMEX-2 experiment. A long-term experiment is also recommended in order to provide a continuous data record of ground-based radiometric measurements covering the SMOS – Aquarius – SMAP era. The resulting data set will support the Level 1C quality assessment for SMOS and SMAP at the accuracy level required for climate applications. In addition, the produced data set will be instrumental for satellite sensor product inter-calibration ensuring an harmonized Level 1 data set of passive microwave observations at L-band for future climate applications.

The objective of DOMEX-3 project is to contribute to the long-term deployment of an L-Band Radiometer at Concordia Station. The activity of the contract is divided in four phases: the first phase deals with the preparation of the instrument and the experiment while the others 3 phases are constituted by the campaign and the analysis of the data acquired during the 4 campaigns 2013, 2014, 2015 and 2016. Phase-1 of the activity was devoted to the preparation of an improved version of the L-band microwave radiometer RADOMEX as well as the definition of acquisition procedure and campaign execution. Phase-1 started in January 2012 and ended in October 2012, the performed activities were reported in the CIP and RR document of the contract [3],[4],[5].

Phase-2 of the activity is constituted by the deployment of the instrument during the first summer Antarctic campaign 2012, the acquisition of the data during 2013 and its analysis and the preparation for the Austral summer campaign 2013. It started in November 2012 and ended in October 2013. Results are presented in the First Year Report of the project [6].

Phase-3 of the activity is the subject of this document, it includes the execution of the Antarctic summer campaign from 2013 to 2016. In particular, this document deals to the description of summer campaign 2016-2017 and the data acquisition and analysis for year 2016.

The different sections of the document describe the execution of the summer campaign 2016 and the analysis of data acquired in 2015-2016. The data acquisition and analysis (D3) is also contained here, the collection of the photographic material is contained in the D4 of the project and the data are contained in D5.

3 The 2016-17 Summer Antarctic Campaign

The third Antarctic campaign of the Domex-3 project was funded by the Italian programme for research in Antarctica - PNRA in the framework of the Monitoring Antarctic Ice Sheet using Advanced Remote Sensing Systems - MAISARS project (PNRA project 2013/AC3.07) leaded by IFAC-CNR. The objective of the project is to investigate on the structure and the properties of the ice sheet at Concordia Station by means of different remote sensing sensors and to inter-compare the obtained results. DOMEX-3 experiment is part of the project.

The 2016 Antarctic campaign of MAISARS involved the substitution of the RF section of the RADOMEX which have been redesigned and modified in the internal calibration system, the removal of GRAIS instrument was installed in 2015-2016 campaign and the execution of radio echo sounding (RES) measurements for measuring sub-surface ice sheet layering by using a GPR system. Conventional maintenance operation were carried out on snow temperature probes consisting of inter-calibration and realignment to their nominal depth.

3.1 Description of the campaign

3.1.1 Activity with the winterover researchers

The winterover responsible of Domex-3 from the end of summer campaign 2016-2017 and which will take care on experiment during 2017 was Laura Caiazzo (University of Florence) who was accurately trained to manage the RADOMEX, to access the internal unit, to download and ship the data. As pointed out in the SoW acquisition plan, angular scans should be extended during the winter and carried out at monthly basis. Laura will setup and check for a nominal instrument functioning. Moreover she will perform routinely snow surveys, for which Laura has been trained by the last winterover Vitale Stanzione during the summer. Routinely snow measurements are summarized as follows:

- daily precipitation particles and fresh snow (daily);
- snow accumulation (weekly);
- superficial snow density: 8 samples at 10 cm below the surface in the surroundings of the snow poles for the seasonal accumulation estimation (bi-weekly)
- first meter snow density at 10 cm steps (monthly).

3.1.2 Activity in the 2016 summer campaign:

2016/2017 Summer Campaign started in November 17 when Francesco Montomoli reached Concordia after a trip started in Italy on 12/11. The second component of the team was Vitale Stanzione, responsible of DomeX experiment during the last winter campaign and already resident at the base.

Figure 3-1: The Summer Campaign Team, Vitale Stanzione (on the left) and Francesco Montomoli (on the right).

During the 35 days spent in Concordia, different activities have been conducted in the context of ESA and PNRA projects.

Concerning DomeX experiment, operations included the maintenance and improvement of the system (Task1 of the SoW [14]) and the setup of the new acquisition plan (Task 2 of the SoW). Main activities are listed below:

- Substitution of the DomeX RF receiver on 25/11. The replacement was mainly motivated by a failure occurred on 5th August in the electrical system of the base, which damaged its thermocontrol unit. Figure 3-2 show an internal view of the RADOMEX where the new receiver (black box behind the PC unit) is already mounted. The main improvement carried out to the new RF receiver was the implementation of a four loads calibration scheme which preserve it from occasional failures of a load and then mitigate the risk of future problem. Technical details are accurately described in [13] and not reported here.

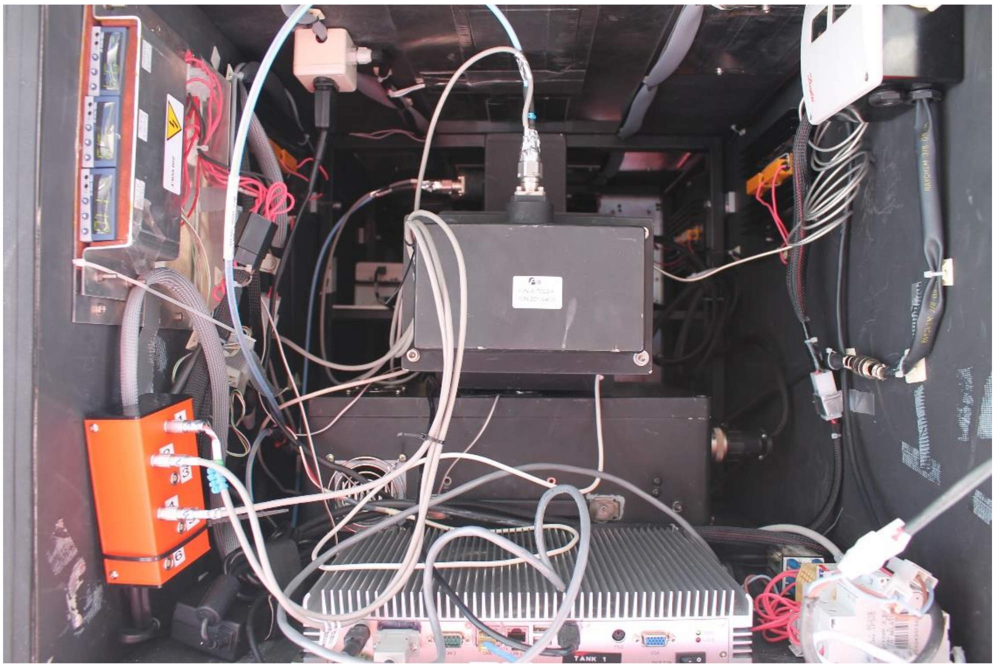

Figure 3-2: internal view of the box containing RADOMEX

- Upgrade of the front panel of the DOMEX designed for a better efficiency in heat dissipation from the interior to the exterior of the radiometer's enclosure during austral summer. The warm air disposal is forced by a circular fan through cylindrical apertures which can be easily opened/closed in the summer/winter period. The fan activation is regulated by a thermostatic system which switches on when the internal temperature exceeds a preset value. A picture of the panel is shown below. Substitution was executed on 1/12/2016.

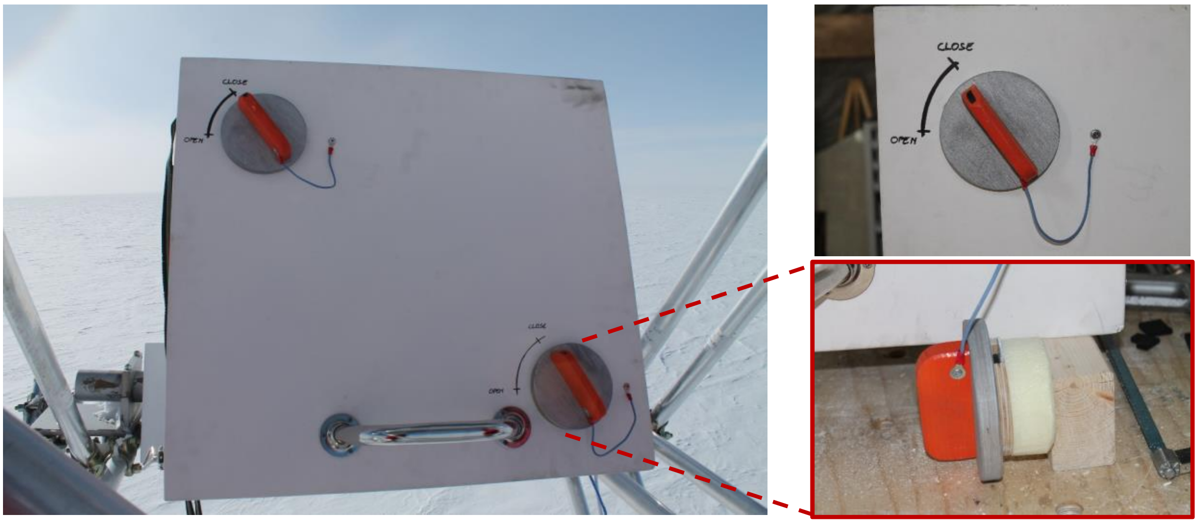

Figure 3-3: view of the new front panel (on the left) showing the details of the aperture system (on the right).

- Angular tests observing brightness temperature at different elevation angles. The first test is performed on snow at daily basis from 20° to 60° with respect to nadir to have an overlapping set of angles for SMOS inter-comparison. The second test spans from 60° to 160° addressed to improve the antenna deconvolution procedure including cold sky for the absolute calibration of the radiometer. The total span (20° to 160°) has significantly increased with respect to the past DOMEX campaigns, providing more accurate and better calibrated measurements. A picture illustrates the different observation angles at 20°, 42° and 160° from left to right.

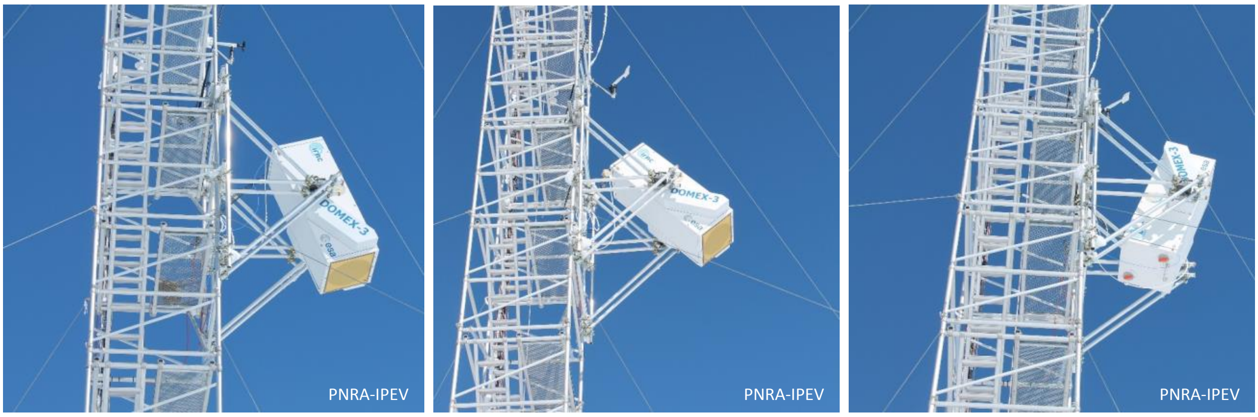

Figure 3-4: RADOMEX observations at 20 deg (left), at 42 deg. (center) and at 160° (on the right).

- Inter-calibration of snow temperature probes and the realignment to their nominal depth from 5cm to 150cm below surface, in Figure 3-5. Realignment was due to snow accumulation during the year. Moreover in the probes area it was registered an anomalous accumulation of 32cm which is more than the double of what measured in previous years. Our interpretation is that the presence of cables which connect probes to the datalogger and actually lying at surface level could accelerate snow accumulation. Preventing future anomalies, all the cables have been lifted up and accurately fixed to the supports, Figure 3-6.

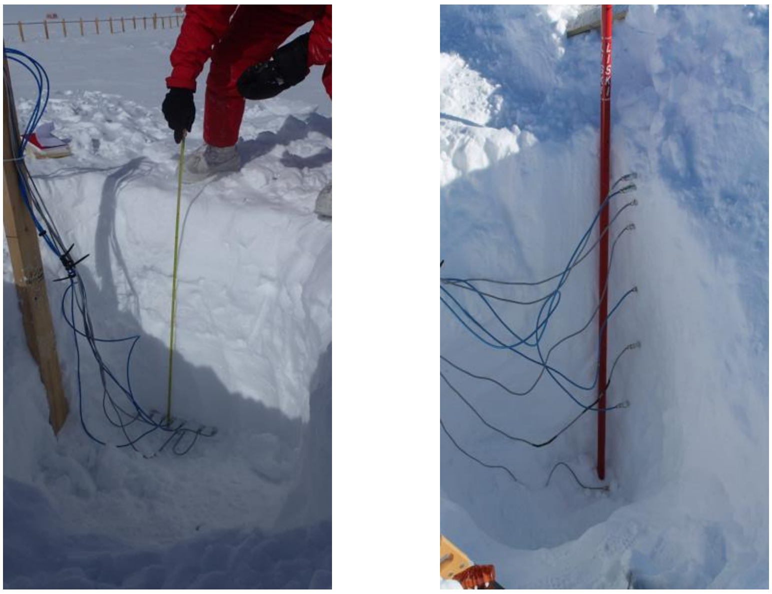

CALIBRATION PHASE MEASUREMENT PHASE

Figure 3-5: Operations conducted on the snow temperature probes including their intercalibration

BEFORE AFTER

Figure 3-6: View of snow temperature probe acquisition area before and after lifting up the cables connecting snow probes to the datalogger

Other activities were devoted to the measurement of snow properties by using Radio Echo Sounders for a better understanding of layering's geometry and give a reference for the interpretation of GRAIS data (ESA-GRAIS project); details are listed below:

- Disassembly of GRAIS antenna from the top of the American Tower on 29/11. The instrument was set up in the past summer campaign and successfully acquired along one year. Data processing and analysis done by IEEC team is currently in progress.
- GPR measurement in an area of around 110m X 100m North-East with respect to the American Tower on 16/12. The instrumentation have been provided by INGV (National Institute Geophysics and Volcanology) during the campaign. The system include a GPR unit GSSI SIR10B which is essentially TX/RX device, the planar antenna operating at 400MHz, the I/O devices and RF cables. Preliminary calibration tests for not moving platform were performed in the area close to the

"spare time tent" in Concordia, then the experiment moved to the investigated area. The area was selected to overlap GRAIS measurement during the calibration phase, in order to add information of snow properties and improve interpretation of the data. Aerial view of the test area and the used acquisition scheme is shown in Figure 3-7. The GPR unit is maintained at warm temperature placed inside a PistenBully PB100 and connected to the antenna sliding on the surface, Figure 3-8.

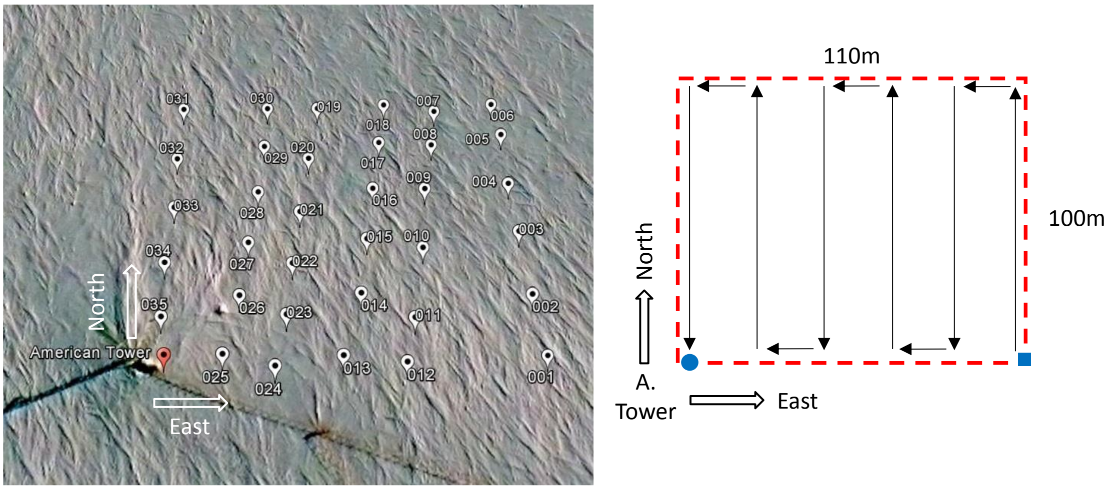

Figure 3-7: View of the area selected for RES measurements (on the left) and the used acquisition scheme (on the right).

Figure 3-8: Measurement set-up for the GPR measurements

The system is well consolidated in the past and extensively used in the determination of snow layering in several parts of the Plateau. It is expected that this data will give a detailed representation of the layerings up to -30m with high accuracy [15].

The summer campaign ended on December 23rd when Francesco Montomoli left Concordia with a Twin Otter flight and arrived in Italy on January 6th.

4 DOMEX-3 - 2016 DATA ANALYSIS

4.1 Data acquisitions

In this section DomeX-3 acquisitions from 1st December 2015 to 1st December 2016 are presented and discussed, with the details of data processing and absolute calibration. The acquisition was continuous over the whole period with some interruptions were occurred on 10/12, 7/1, 26/1, 18/2, 9/6, 12/6, 6/8, 18/11. Interruptions were mainly caused by several blackouts occurred in electric system of the base, while the instrument itself acquired correctly. Most of the interruptions did not affect the nominal functioning of the system and it automatically rebooted with the standard setup. Nevertheless, an important failure event which occurred after 6/8 blackout compromised the thermo-controlled unit of the receiver affecting the Tb in the form of anomalous oscillation. A method to correct anomaly have been implemented and applied in the post processing phase, while no significant action was possible on the receiver until the instrumental change in summer. The damaged components will be better identified at IFAC laboratories once dedicated tests will be performed.

An amount of 3002340 samples, corresponding to 96.8% of total acquisitions are currently available. The RADOMEX worked with two different calibration types, total power (TP) using hot and cold loads from 1/12/2015 to 29/3/2016 and from 4/7/2016 to 24/11/2016, and TP using hot load and the noise source (NS) from 29/3/2016 to 4/7/2016.

Acquisition schedule is listed in Table 4-1. Angular scans were repeated in 19-23 Dec 2015 and 12-19 Jun 2016 pointing between 30° and 115° with respect to nadir; clear sky calibrations were performed on 19-23 Dec. 2015, 22-29 Jan. and 9-12 June pointing at 115°. In addition, during the 2015 Summer Campaign RADOMEX was moved at 30° and 45° during 4 days, for inter-comparison with the UWBRAD radiometer in the cal/val activities [7]. In the remaining days the observation angle was nominal at 42°.

Table 4-1: Data acquisition schedule for Dec 2015- Dec 2016

ACQUISITION TYPE	VALUE [deg] (MIN/MAX/STEP)	FROM/TO	CAL. TYPE
Angular scan #1	30/120 step 10	15-19 Dec 2015	TP
Angular scan #2	30/115 step 5	12-19 Jun 2016	NS
Clear SKY #1	115	19/12 - 23/12	TP
Clear SKY #2	115	22/1 - 29/1	TP
Clear SKY #3	115	9/06 - 12/06	NS
UWBRAD	30/45	24/12 - 29/12	TP
Nominal Angle	42	elsewhere	TP/NS

4.2 Data processing and calibration

4.2.1 Reconstruction of corrupted data

The first version of data, so called "raw data" in the rest of the document, is shown in Figure 4-1 as average and standard deviation values. Here the TB is averaged every 20 samples without thermal corrections or absolute calibration /pattern deconvolution. It can be observed that:

1. From (December 1st 2015 - August 6th 2016) acquisitions were continuous and the Tb is consistent with the past year. Receiver temporal stability is also confirmed by low standard deviation, was computed over 20 acquired samples, which ranged from 0.15-0.25K for both V and H pol. for the whole period.
2. From (August 6th -) Tb exhibits anomalous fluctuations reaching to 1K standard deviation in the worst case (average is 0.12K), degrading accuracy of the data.

The problem have been investigated in depth observing the voltages (in digital counts) measured at the end of the receiver chain (Ccold, Chot, CV,CH) and the other telemetry data, namely all the PT100 values which are measured at different sections of the receiver. A typical behavior after the failure event is the one shown in Figure 4-1 selecting a relatively short period from 20 to 27 Sept. From a qualitative analysis, oscillations are evident in the four channels but they are not persistent for the whole day. In fact the values remain stable for several hours/day with normal functioning, then they rapidly fluctuate in a systematic way. For the same period we reported values of 4 temperature probes in Figure 4-2, among which three are located inside the receiver namely on the switch, on the calibration loads and on the internal cable (represented in orange, green and grey respectively), and the last one is placed in the antenna cables outside the receiver (blue line). In this last section PT100 values are not affected by fluctuation, whether they smoothly changes as a function of the internal temperature in a nominal way. It must also be considered that PT100 of the two sections are powered independently and stabilized by two different devices. That is sufficient to exclude a real change of the physical temperature inside the instrument and to address the problem to the receiver section.

Looking inside the receiver, it must be observed that anomalous fluctuations of temperature are registered from PT100 both in the switch and in the hot load see Figure 4-2, which are independently stabilized in temperature but they are feeded by the same supply. It is then reasonable to exclude a direct damage of PID system of the thermo regulated part of the radiometer, and to address it to the failure of an electric component (diodes or transistors) which resides in the power stabilization of the receiver. However, this explanation must be confirmed by the test which will be performed in IFAC laboratories in the forthcoming weeks. Moreover, it must be observed that fluctuations on Tb are timely correlated with physical temperature of the RF section measured outside the thermo-controlled box as in Figure 4-8 . In practice, the oscillations disappeared when the temperature is below a certain value. In view of these considerations, to lower the temperature of the receiver and limit the number of fluctuations, we decided to open the rear panel of RADOMEX enclosure. Operation were planned at IFAC and performed by winterover Vitale Stanzione on October 6th.

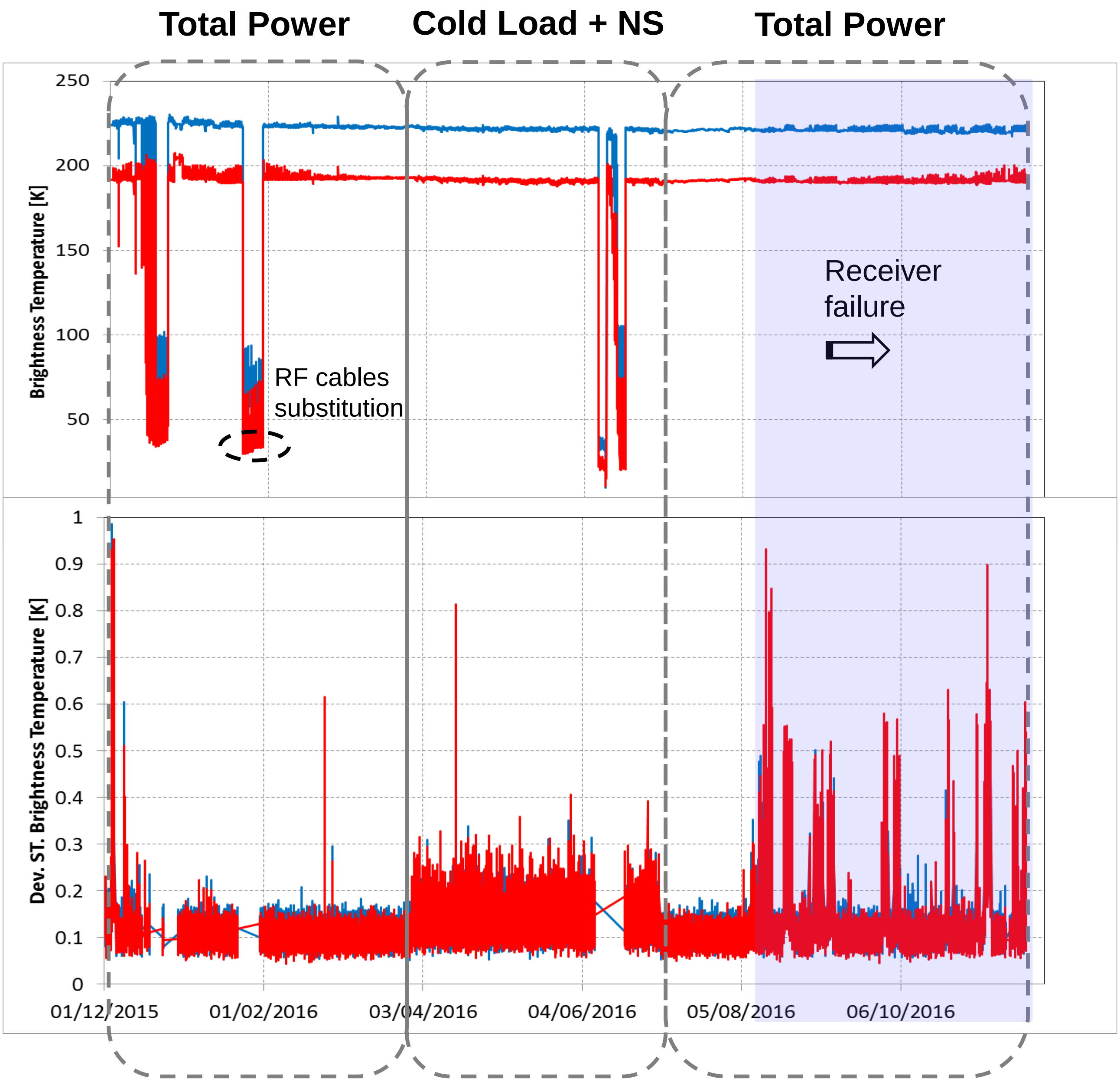

Figure 4-1: Brightness temperature average (up) and standard deviations (down) of "Raw data" over 20 samples

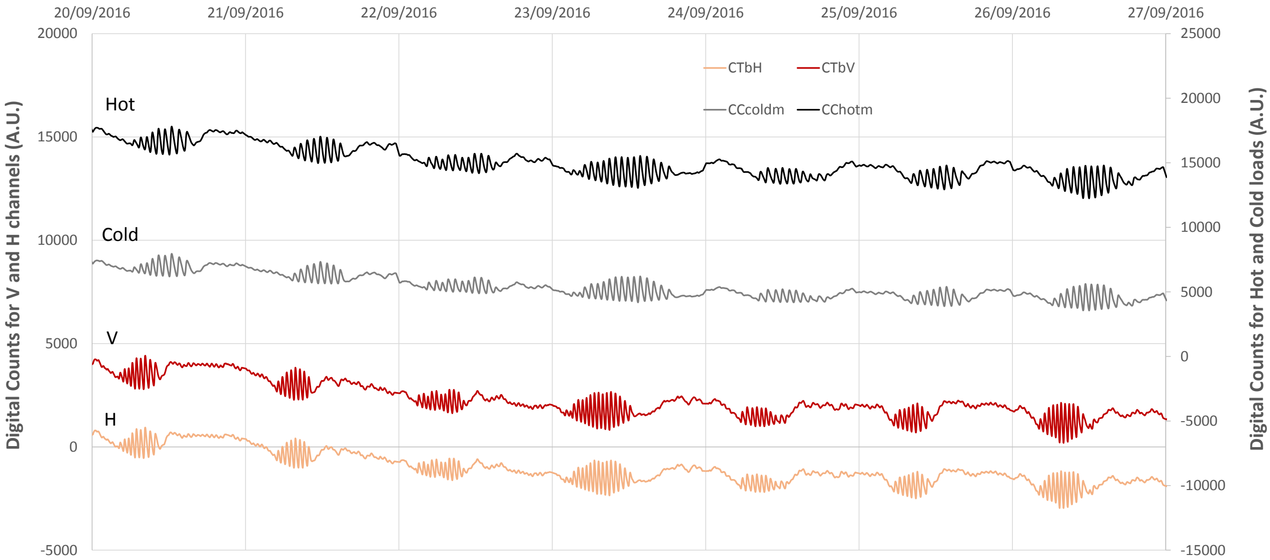

Figure 4-1: Digital counts of the four radiometric channels in the period 20-27 September. Each channel is identified by a different colours: V channel (red), H channel (rose), Hot load (black) and Cold Load (grey).

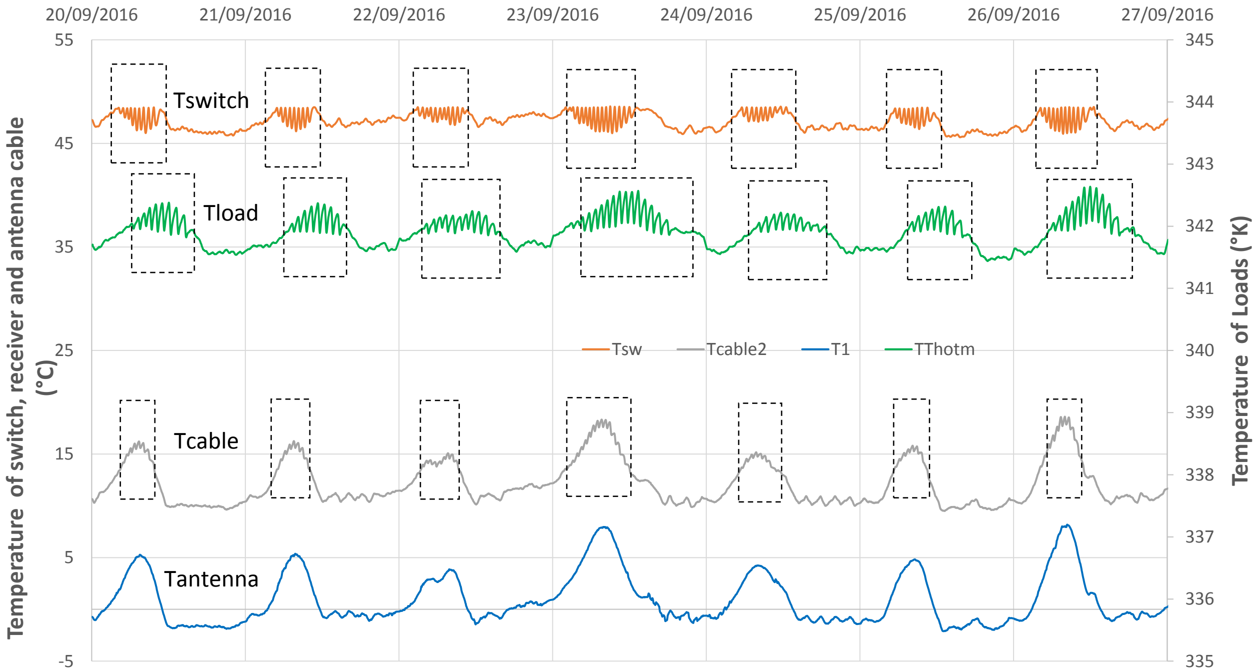

Figure 4-2: Values from PT100 probes in the period 20-27 Sept. Probes are placed at different sections of the radiometer, at the switch (orange), at cold load (green) at the internal cables (grey) and at the antenna cables (blue).

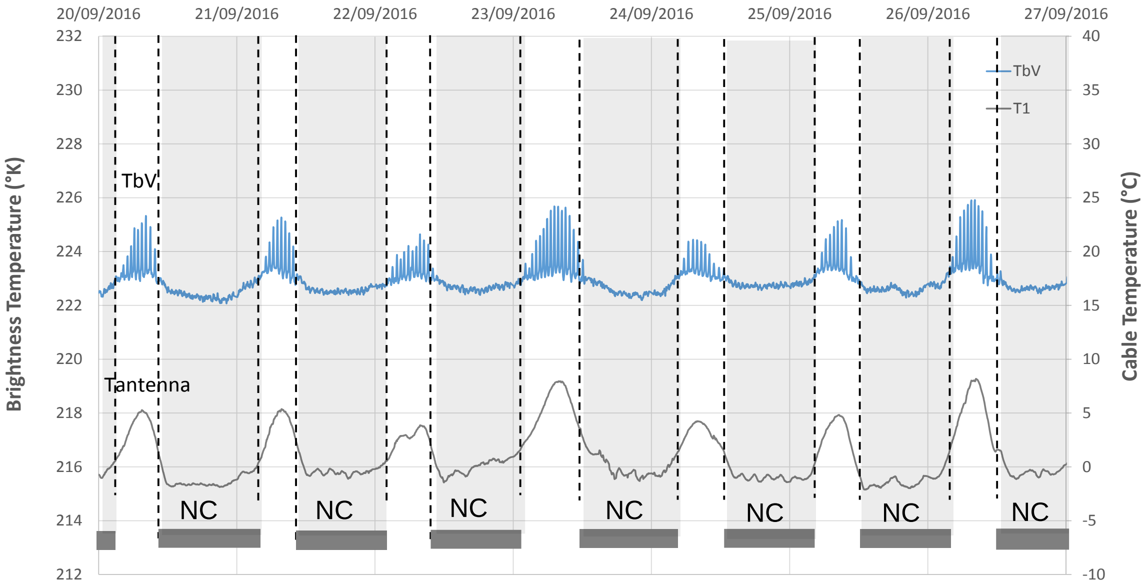

Figure 4-3: Brightness temperature at V- pol (blue) and antenna temperature (grey) of a selected period after the failure. Grey bars show the not corrupted data samples (NC).

Corrupted data from 6/8 to 24/11 were filtered out using a comparative threshold on the cable temperature T1. The obtained value which ensure the removal of Tb fluctuations and to keep the previous accuracy on Tb (Tb std< 0.25K) was T1<=-1°C. Data are deleted wherever the condition is not met. Although this condition can provide data with a good quality, it caused a considerable loss of data (only keep 13% of the total) which is then reduced after the panel aperture (26% of the total are available). The Tb values reported before and after the filtering are shown in Figure 4-4.

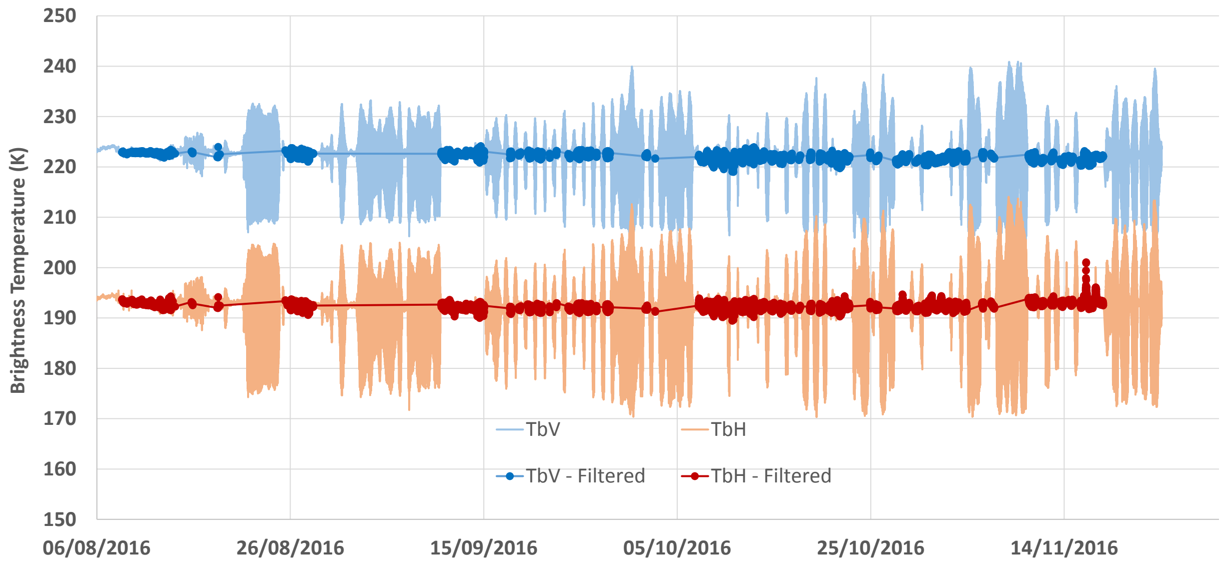

Figure 4-4: TB at V and H pol from 6th August, before and after the filtering

4.2.2 Tb correction for thermal variation

Brightness temperature have been corrected from the effect of day/night thermal gradient which affect the electromagnetic properties of lossy devices like cables and connectors, which are placed outside the thermo controlled box. The resulting effect is in the form of a modulation on Tb amplitudes which is governed by the daily fluctuations of physical temperature inside the instrument, as shown in Figure 4-6 for two different period of the season, in early summer and late summer. The summer fluctuations are mainly caused by sun heating which is maximum at around midday and minimum during the night when the sun is still present above the horizon but with lower intensity. Temperature fluctuations disappeared in winter when the sun is not present and the thermal regulation inside the instrument is performing better.

The mitigation of the thermal effects is based on a consolidated procedure which have been pointed out in the previous annual reports [6], [7].

The correction algorithm is based on the minimization of Friis formula [7] calculated along the receiving chain from the antenna frontend to the input of the thermo controlled section. The main steps are hereinafter summarized:

1. Realignment of Tb and cable temperatures from thermal delays
2. Calculation of Friis formula from the antenna to the switch port, placed in the thermo regulated box. To compute the formula we identified two different sections, one colder located near the antenna section and one hotter, placed inside the RF section near the switch. A schematic representation is shown in Figure 4-5. Physical temperatures are obtained from PT100 probes placed on the antenna cables for the first section (identified with T1 and T2 for V and H pol.), and on the internal cables for the second section (i.e. inside the receiver), here called Tcable1 and Tcable2. The losses will be then identified with L1 and L2.

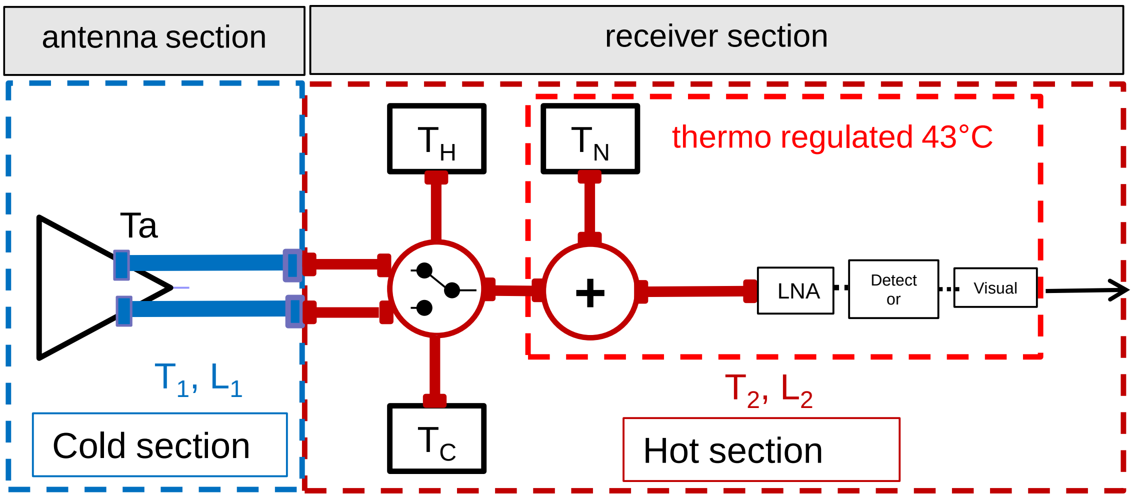

Figure 4-5: Block diagram of the RADOMEX architecture including the "cold section" and the "hot section".

3. Minimization was on Tb standard deviations with respect to L1, L2 observing the following rule: 24H/day for V-pol, and only sun minimums for H-pol.

The procedure iterated every 4 days over the whole year. An example of TbV before and after the correction is shown in Figure 4-7 covering two different periods with distinct thermal conditions, namely at the beginning of summer (Dec. 2015) and at the end of the summer (Feb-Mar 2016). Thermal correction works well in both cases leaving small residual oscillations on the order of +/- 0.5K. Decorrelation with physical temperatures is highlighted in the scatterplot of Figure 4-8, where the determination coefficient drops from 0.97 to 0.01.

Estimated values of L1, L2 for V- and H- polarization are plotted on Figure 4-9 and Figure 4-10 together with their physical temperature in the secondary axis. A good correlation between L1-L2 with temperatures is observed and confirmed by diagrams of Figure 4-11, showing an inverse relationship (L increases when temperature decreases, meaning lower losses). Moreover, it should be clarified that L is a cumulative loss, namely the sum of losses of single devices from the antenna to the switch and takes into account possible modification of mismatches which also leads to a difference in the measurements. Values are summarized in Table 4-2.

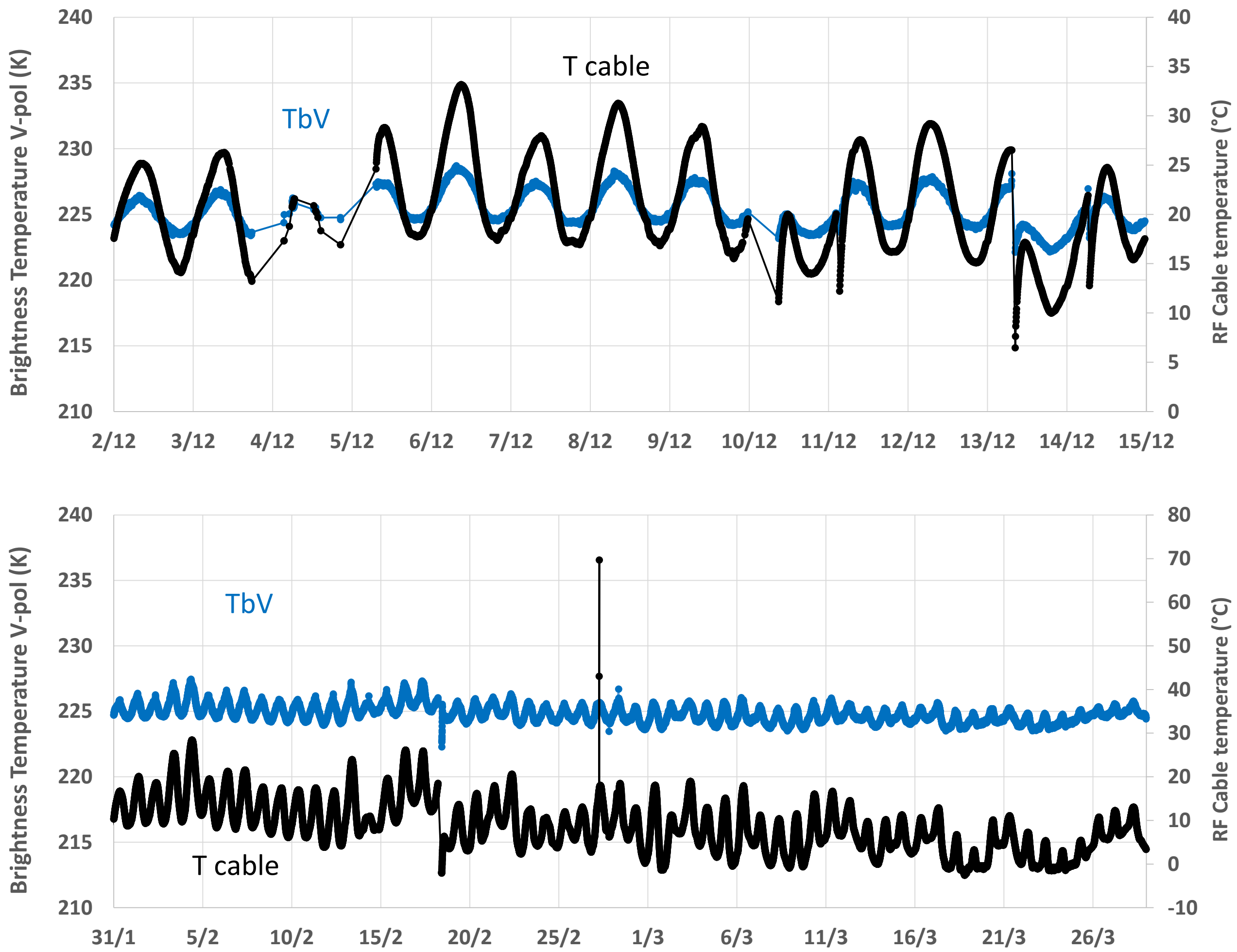

Figure 4-6: Brightness temperature and Cable temperatures in two different periods: in early summer (top) and late summer (bottom).

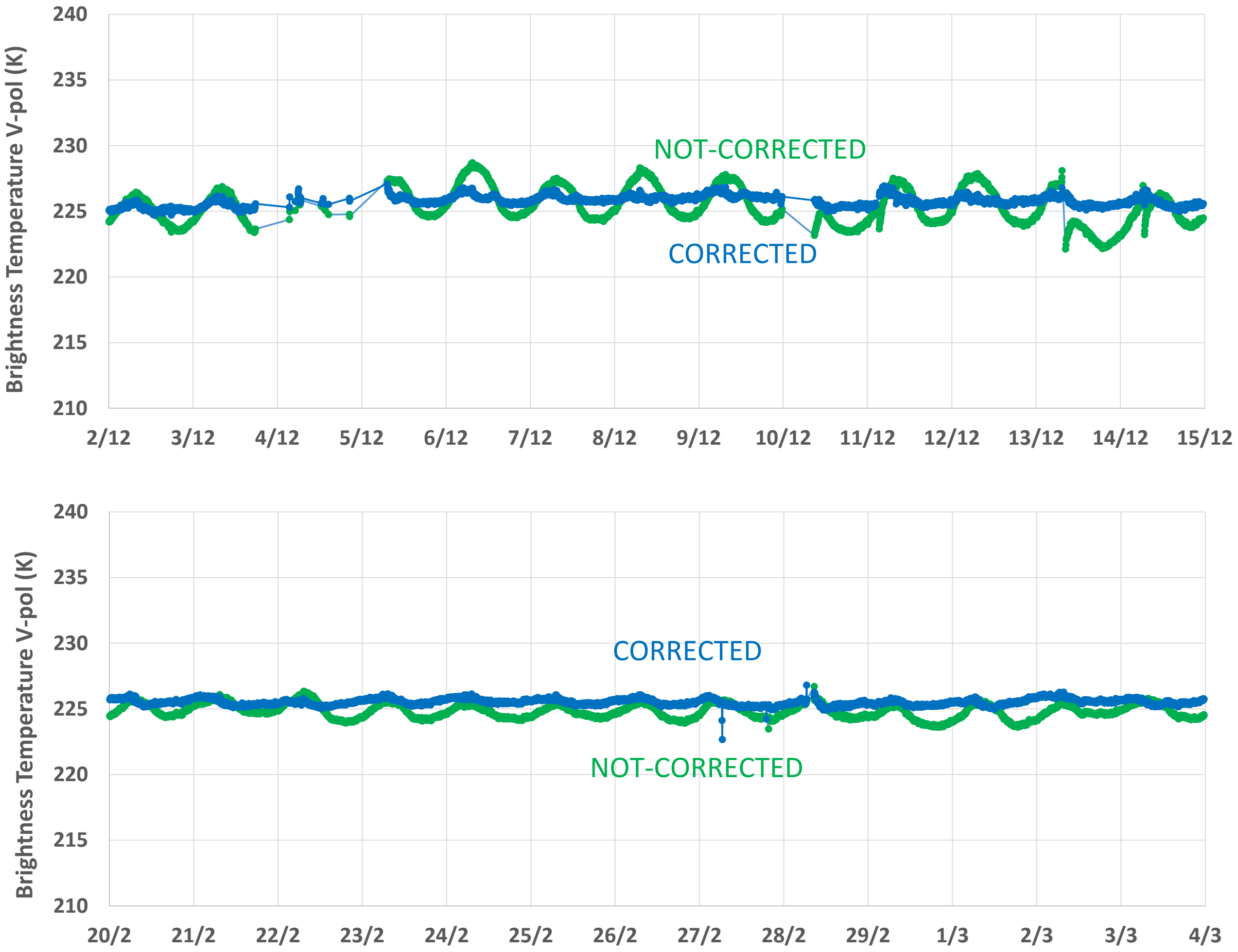

Figure 4-7: Brightness temperature at V- pol, before and after the correction for early summer (top) and late summer (bottom).

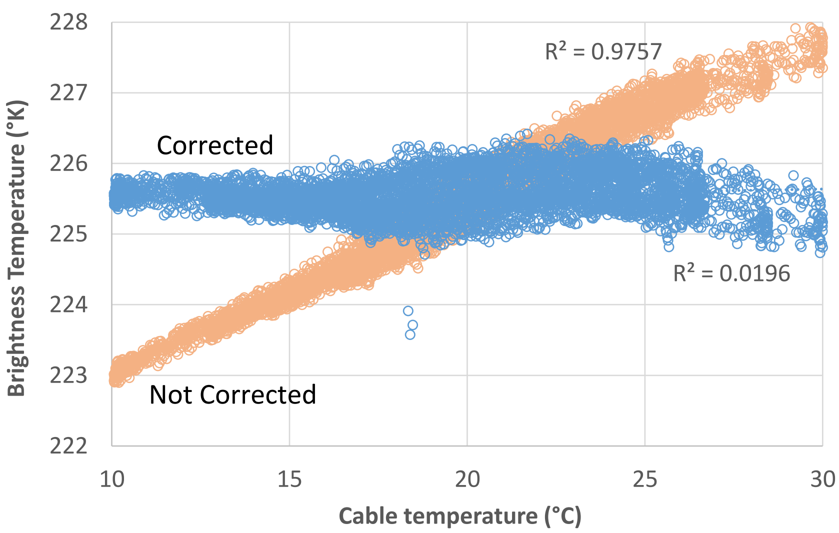

Figure 4-8: Correlation between Tbv and cable temperature T1, before the correction (orange) and after the correction (blue).

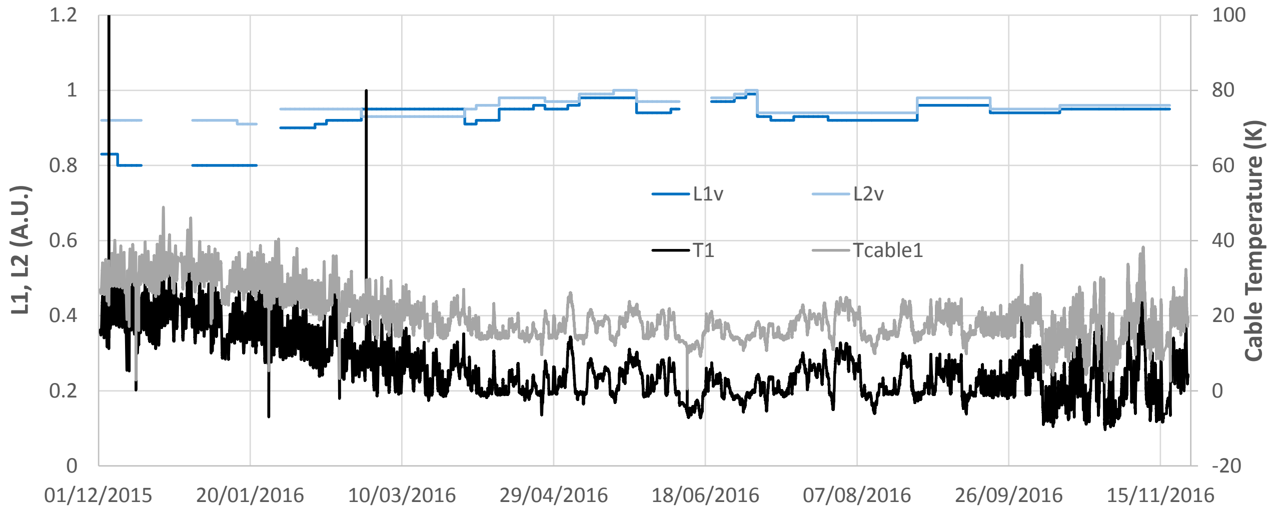

Figure 4-9: temporal estimation of L1, L2 for the V- pol channel (left axis) and cable temperatures (right axis).

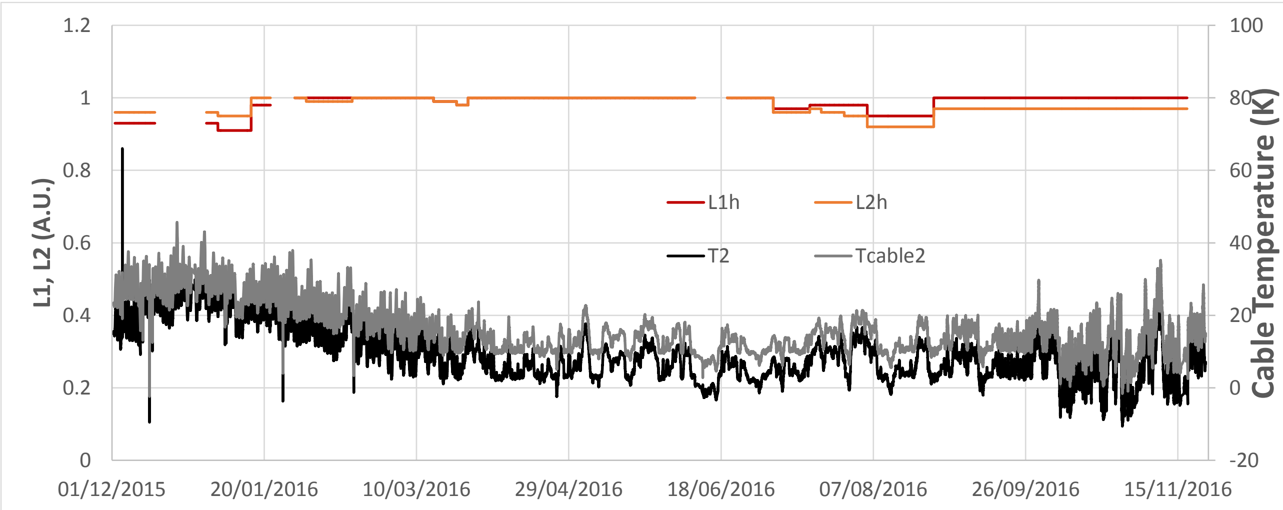

Figure 4-10: temporal estimation of L1, L2 for the H- pol channel (left axis) and cable temperatures (right axis).

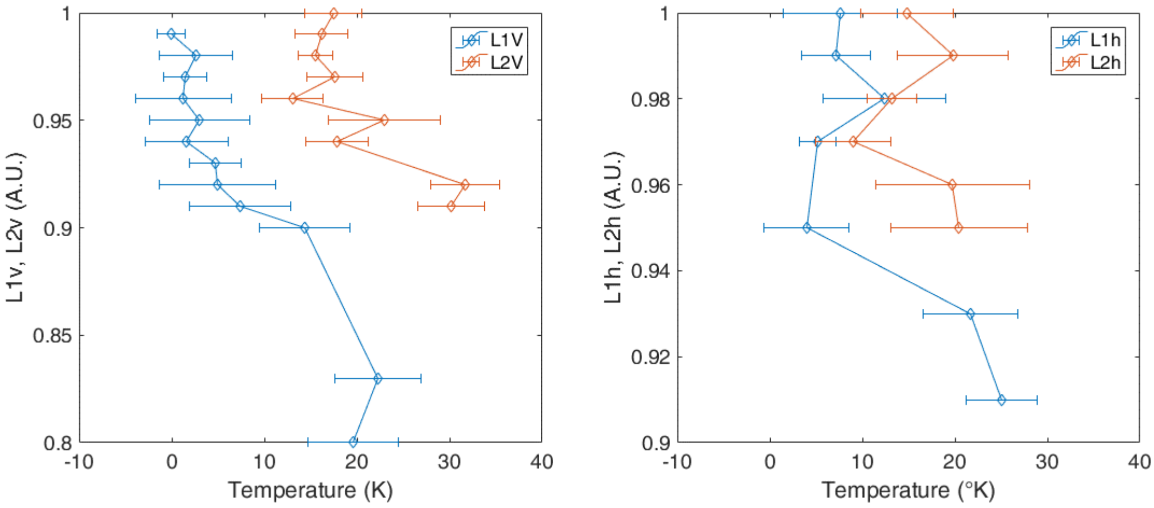

Figure 4-11: Estimated values of L1,L2 as a function of cable temperatures, for V-pol channel (left) and H- pol channel (right).

Table 4-2: L1 and L2 values for V and H pol.

date (From/To)	Tcable1	Tcable2	T1	T2	L1v	L1h	L2v	L2h
02/12/2015 - 07/12/2015	28.09	24.69	17.57	16.99	0.83	0.93	0.92	0.96
07/12/2015 - 04/01/2016	35.75	32.92	27.31	21.74	0.8	0.93	0.92	0.96
04/01/2016 - 15/01/2016	27.76	24.44	14.67	19.72	0.8	0.91	0.92	0.95
15/01/2016 - 30/01/2016	27.99	24.71	15.24	20.12	0.8	0.98	0.91	1
30/01/2016 - 02/02/2016	23.52	19.90	9.90	13.48	0.9	1	0.95	1
02/02/2016 - 10/02/2016	22.70	18.91	9.29	12.55	0.9	1	0.95	0.99
10/02/2016 - 17/02/2016	28.79	25.50	16.90	19.73	0.91	1	0.95	0.99
17/02/2016 - 25/02/2016	25.02	21.43	12.14	15.59	0.92	1	0.95	1
25/02/2016 - 15/03/2016	21.53	17.75	7.85	11.12	0.95	1	0.93	1
15/03/2016 - 23/03/2016	17.68	13.61	3.61	7.38	0.95	0.99	0.93	0.99
23/03/2016 - 26/03/2016	16.38	12.20	1.33	5.06	0.95	0.98	0.93	0.98
26/03/2016 - 30/03/2016	20.08	16.19	6.16	9.98	0.95	1	0.93	1
30/03/2016 - 03/04/2016	19.79	15.93	6.33	9.90	0.91	1	0.95	1
03/04/2016 - 11/04/2016	15.16	10.93	0.83	4.20	0.92	1	0.96	1
11/04/2016 - 22/04/2016	14.24	9.93	-0.82	2.61	0.95	1	0.98	1
22/04/2016 - 26/04/2016	17.91	13.86	3.98	7.67	0.96	1	0.98	1
26/04/2016 - 03/05/2016	20.00	16.17	6.14	9.85	0.95	1	0.97	1
03/05/2016 - 07/05/2016	22.97	19.31	10.20	13.69	0.96	1	0.97	1
07/05/2016 - 18/05/2016	14.43	10.15	-0.68	3.08	0.98	1	0.99	1
18/05/2016 - 26/05/2016	13.04	8.61	-1.89	1.90	0.98	1	1	1
26/05/2016 - 06/06/2016	22.83	19.15	9.98	13.46	0.94	1	0.97	1
06/06/2016 - 20/06/2016	18.97	14.96	5.22	8.99	0.95	1	0.97	1
20/06/2016 - 27/06/2016	20.42	16.62	6.23	10.32	0.97	1	0.98	1
27/06/2016 - 01/07/2016	13.98	9.65	-1.80	1.86	0.98	1	0.99	1
01/07/2016 - 05/07/2016	13.53	9.19	-1.95	2.31	0.99	1	1	1
05/07/2016 - 09/07/2016	17.82	13.79	3.55	7.80	0.93	0.97	0.94	0.96
09/07/2016 - 17/07/2016	17.82	13.79	3.70	8.15	0.92	0.97	0.94	0.96
17/07/2016 - 28/07/2016	18.40	14.43	4.48	8.69	0.93	0.98	0.94	0.97
28/07/2016 - 05/08/2016	17.60	13.45	3.50	7.21	0.92	0.98	0.94	0.95
05/08/2016 - 26/08/2016	21.83	18.08	8.94	12.91	0.92	0.95	0.94	0.92
26/08/2016 - 19/09/2016	13.57	9.15	-2.33	1.97	0.96	1	0.98	0.97
19/09/2016 - 12/10/2016	15.09	10.54	-1.04	3.39	0.94	1	0.95	0.97
12/10/2016-24/11/2016	12.97	8.63	-2.59	1.03	0.95	1	0.96	0.97

4.2.3 Absolute Calibration

The last step of data processing was the absolute calibration. Data are not deconvoluted, but a new update with improved deconvolution will be provided after the elaboration of 2016 Summer campaign data.

Absolute calibration was performed by using as reference the clear sky observed at 115° (i.e. the maximum reachable angle) and the average Tb value measured on snow in winter time at 42° of incidence angle for the previous year. As discussed in the previous document [7] observations at 115° are not fully representative for cold sky since the Tb is contaminated by snow contributions which are detected by the side lobes of the antenna. Moreover it was not possible to reach to steeper angles until beginning of Dec. 2016, when the radiometer was manually moved upwards to 160 degrees. Calibrated Tb for clear sky acquisitions performed in Dec 2015, Jan-June 2016 is shown in Figure 4-12. The highest peaks in figure are due to the presence of the sun in the antenna pattern, while the smallest peaks (about 10K) occurred because of the crossing of the galactic plane. A more irregular trend is observed in June, which is expected since the calibration was with the noise source mode. An unexpected fluctuation on H- pol occurred on 25 and 26 January while disappearing after the change of RF cables in 26th January. It is then reasonable that the fluctuation derived from the H- pol cable, but we have few evidence for a possible explanation. The normal functioning was replaced after the cable substitution. Average values of the calibrated sky observations are indicated on Table 4-3.

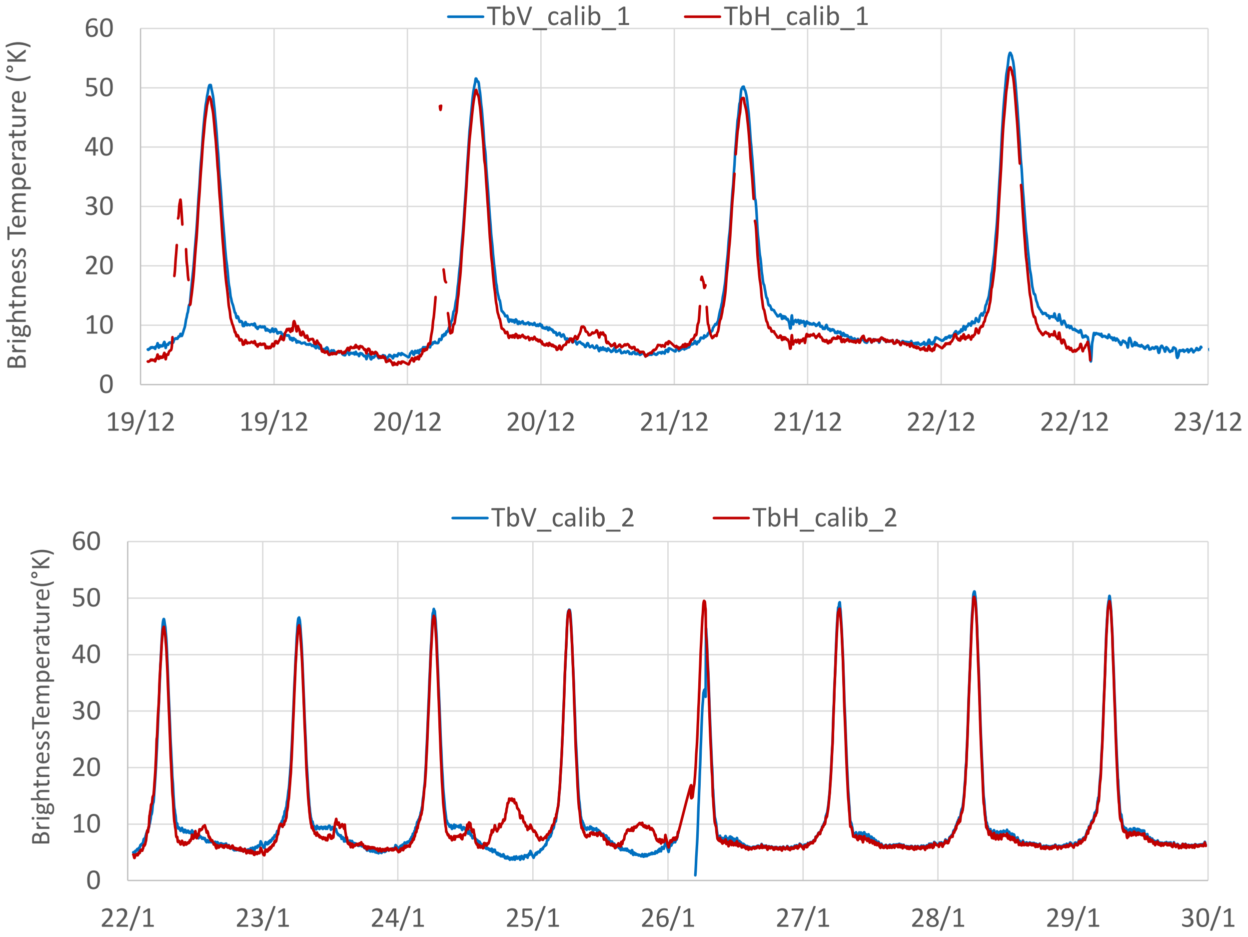

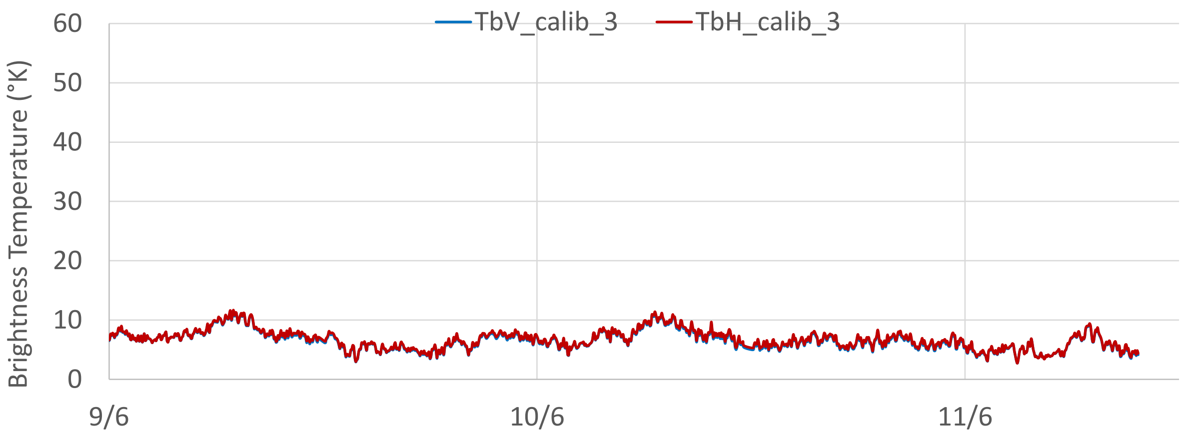

Figure 4-12: Clear sky observation at 115 deg. Plots represent the TbV and TbH for different acquisitions: (up) Dec 2015, (middle) Jan 2016, (down) June 2016. In the last one the highest peaks are due to the cross of the galactic plane.

Table 4-3: Average values of clear sky observation when removing the direct contribution from the sun

	TbV (K)	Std (K)	TbH (K)	Std (K)	Inc. Angle (deg)
Dec 2015	6.4	0.09	6.6	0.09	115
Jan 2016	6.03	0.08	6.03	0.08	115
Apr 2016	6.5	0.1	6.6	0.1	115

4.3 Data Analysis

Brightness temperature of calibrated data is shown in Figure 4-13 at V and H polarization. The time series from 1/12/2015 to 24/11/2016 contains data averaged every 3.33 minutes for acquisitions at 42 deg. and clear sky observations, every 50 seconds for the angular scan to ensure a better separation between nominal observations and transitional angles. The amount of data delivered to ESA are 107645 samples corresponding to around 71% of available ones. The remaining part were filtered out after the failure on August 6th.

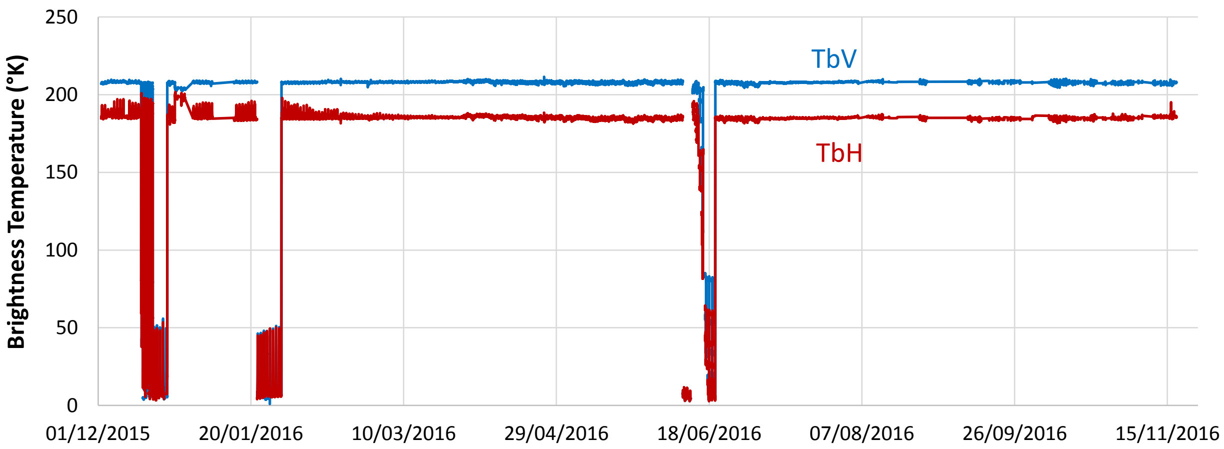

Figure 4-13: Calibrated brightness temperature of 2015-2016 acquisitions

Data acquired at 42 degrees are shown in Figure 4-14. Peaks of several kelvins above the average occurred from December to March, only at H polarization due to the sun contribution at L-band which is reflected by the surface layers of the snow. Avoiding sun reflection for better understanding of the physical processes among the firn, a new representation when the sun is out of the antenna pattern is given in Figure 4-15 and its standard deviation of each observation in Figure 4-16.

Nominal acquisitions at 42 degrees confirm the temporal stability at V polarization with average and standard deviation of 207.9K and 0.55K respectively, as in Figure 4-16. A similar behavior is observed for H-pol (mean=184.9K and std=0.72K) with no evident change due to a modification on snow layers, as occurred on 2015. The histograms of calibrated V and H pol. showing the data distribution at 42 deg. is reported in Figure 4-17.

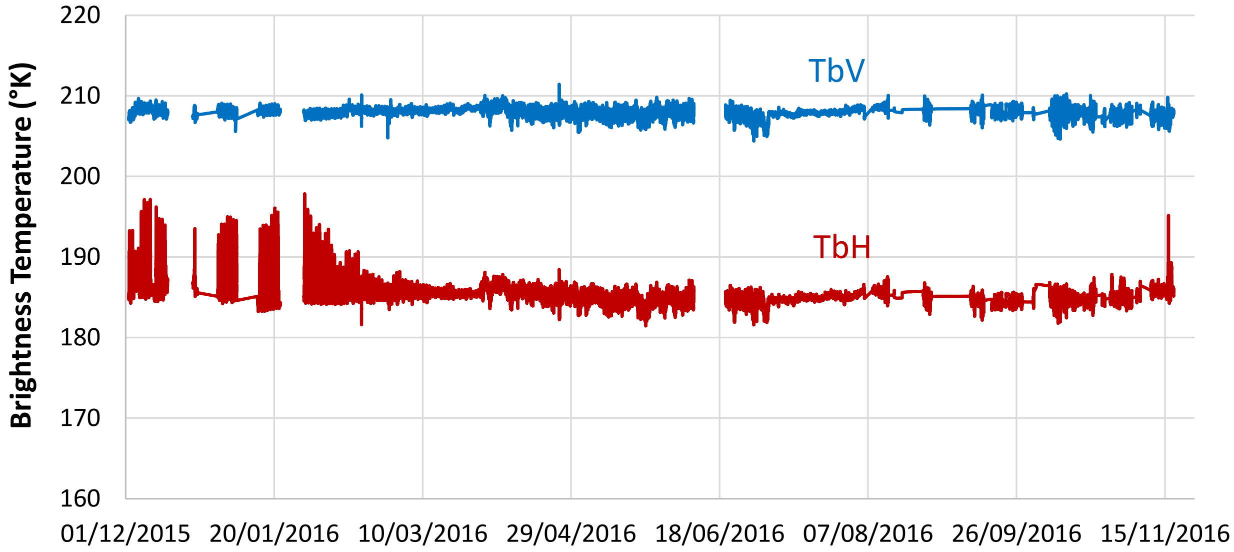

Figure 4-14; Brightness temperature recorded on 2016 for V- pol (blue) and H- pol (Red) at 42° observation

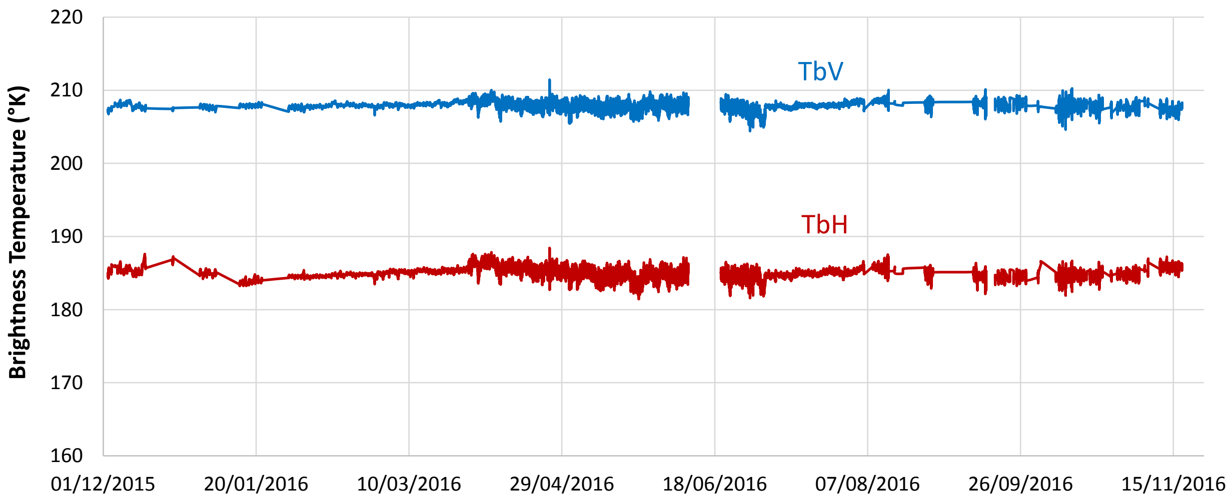

Figure 4-15: Brightness temperature at 42° after the removal of the effect of sun reflections.

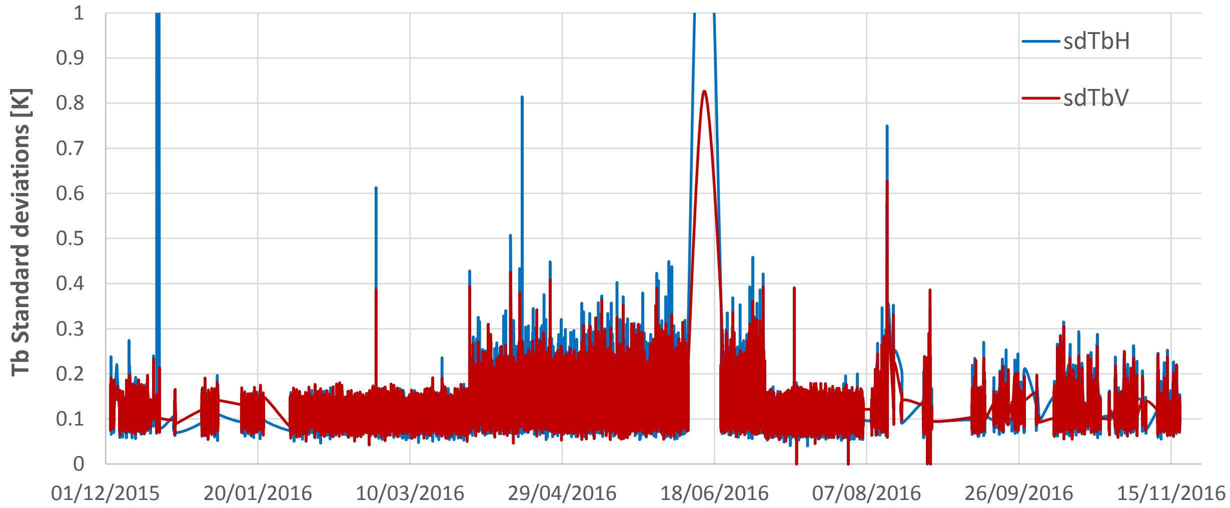

Figure 4-16: Brightness temperature std. after the data processing.

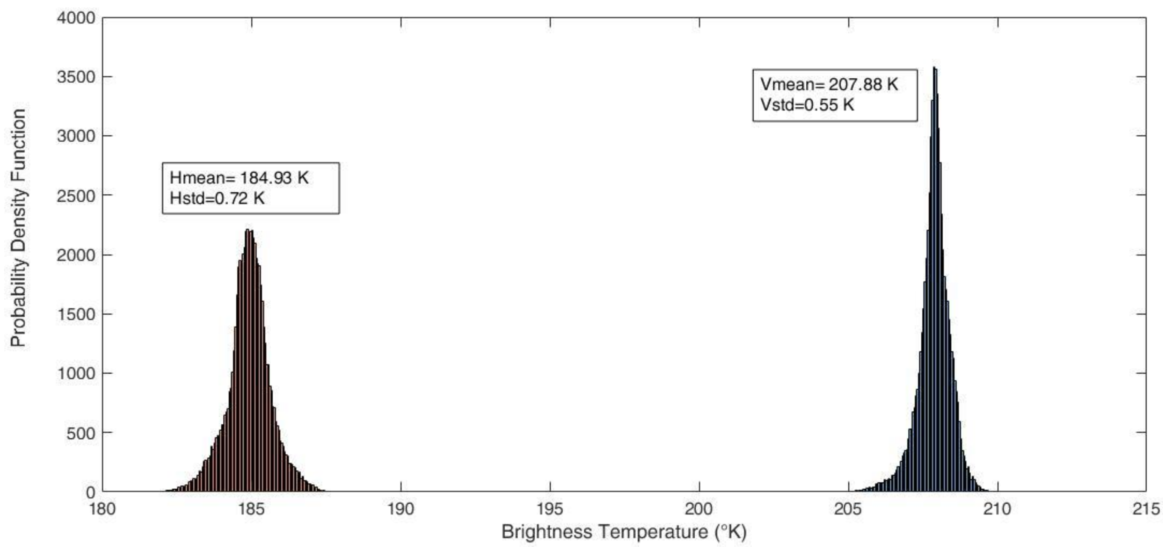

Figure 4-17: Statistics of calibrated TbV and TbH showing the probability density function of data acquired along the year. Average and standard deviations are reported on the plot.

The polarization index PI (PI = 2* (Tbv-Tbh)/(Tbv+Tbh)) is represented in Figure 4-18. PI shows some variation in the summer until 30 Jan which are mainly due to the modification of H-pol. The average value of the PI along the year is 0.116 and is slightly higher than the one observed in 2014 and 2015 (0.110 and 0.108 respectively). The standard deviation of the PI is 0.0024 K, which is much better if compared with the 2015 one (std=0.012) and very similar to what observed on 2014 (std=0.0028).

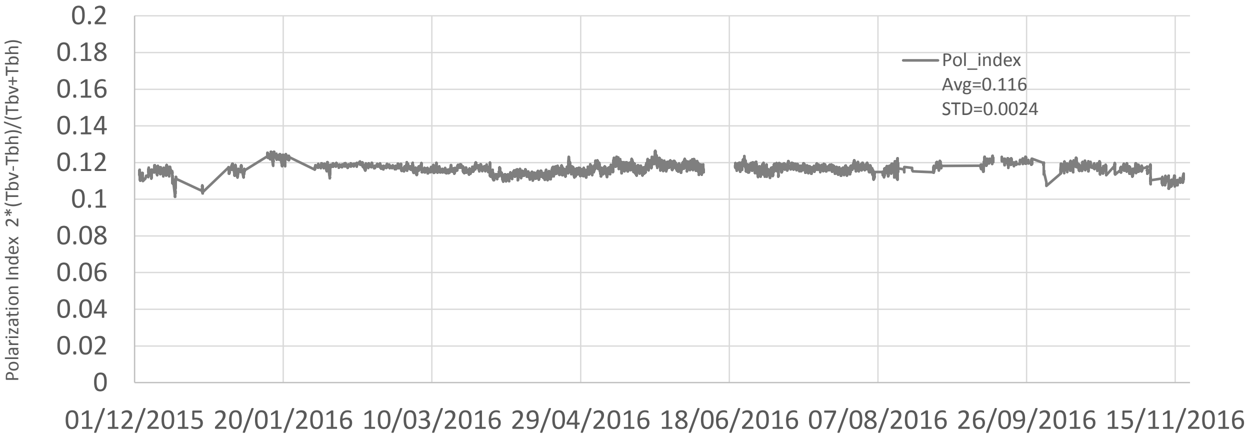

Figure 4-18: Polarization index as a function of time

The physical temperature series of inside the thermo-controlled section is given in Figure 4-19, measured by PT100 placed over the switch (red line) and on the noise source (blue line). Several spikes during the summer are the consequences of electrical blackouts, which interrupted the acquisitions and cooled down the system. The oscillations after August 6th failure are more evident for both lines whereas the PID lost the thermal control. Temperatures measured on the RF cables at the antenna and the receiver sections (at V-channel), are shown in Figure 4-20. Both temperature fluctuates +/- 10 °C with respect to their mean value which is governed by the seasonal variation inside the radiometer. Fluctuations are more stable in winter, because the temperature can be controlled internally at around 0°C. An average decrease is observed after the opening of the panel, in October 6th.

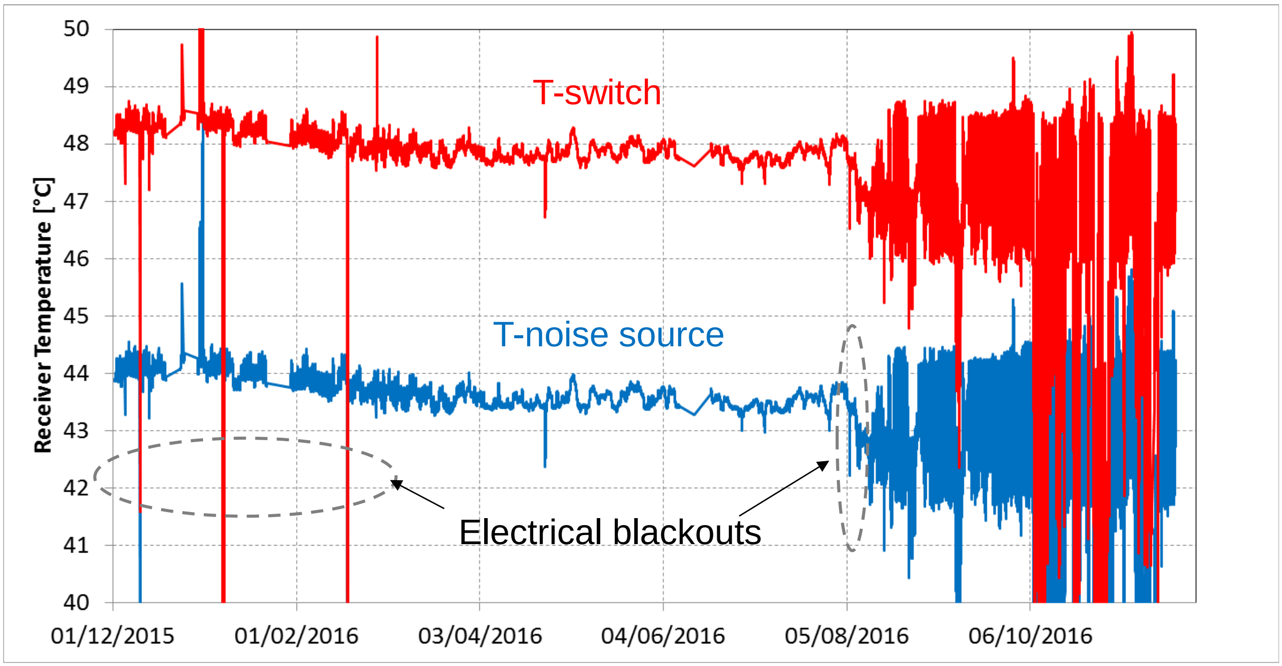

Figure 4-19: Physical temperature measure by PT100 inside the thermo-regulated box, on the switch (red) and on the noise source (blue).

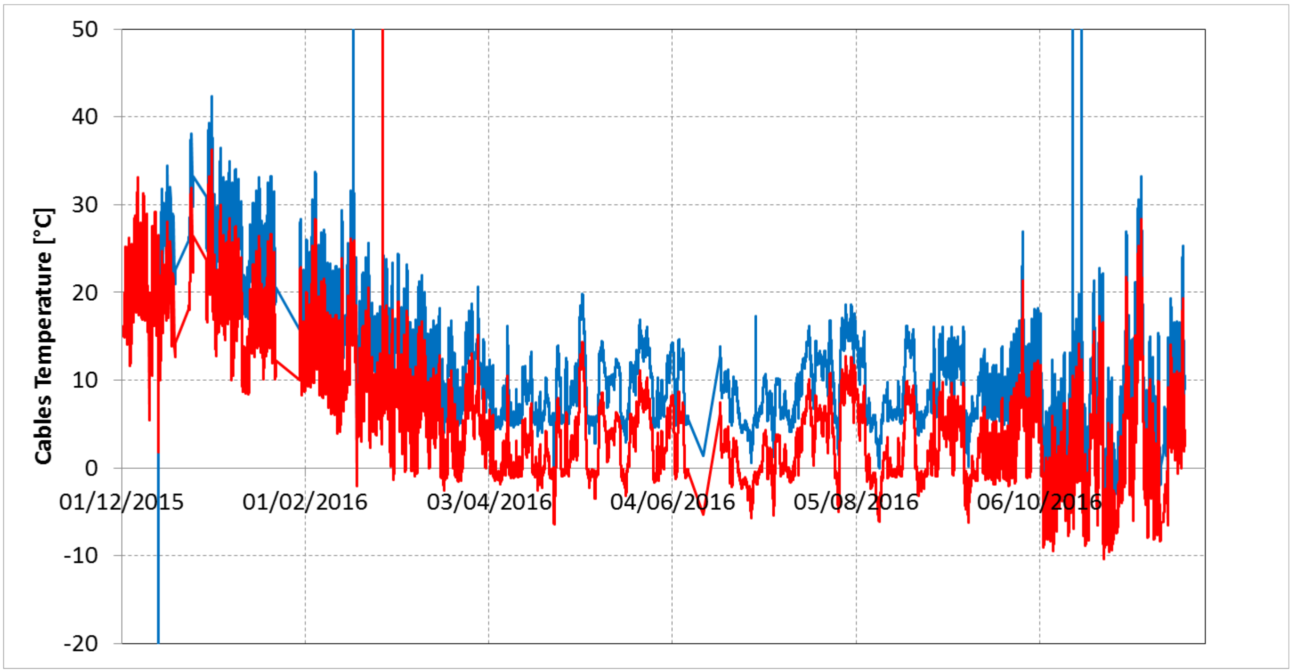

Figure 4-20: Temperature measured on the antenna cable (red) and on the RF cable (blue)

4.3.1 Antenna cable substitution

On January 26th the RF cables which connects the antenna to RF receiver frontend were substituted. The new coaxial cables, manufactured by Times Microwave LTD, are the Phasetrack 210 equipped with N-type connectors. The main improvement is the lower sensitivity to temperature variations than the previous RG-142. A picture of the new cables with the details of internal structures is shown in Figure 4-21. The better performances are related to their phase characteristics as a function of the operating temperature, which is more flat and constant with respect to the old PTFE, as explained in the comparative analysis in Figure 4-21. This means that the electrical length (and so the adaptation) and the insertion losses should remain more stable during the whole acquisitions.

The frequency response of the reflection coefficient of the new cables measured in the IFAC laboratories is reported in Figure 4-23 in the amplitude (left) and phase (right) characteristics and compared with the old ones. A lower S11 over the whole bandwidth is the indication of a general better adaptation.

The uncalibrated brightness temperatures before and after the substitution is shown in Figure 4-24. A general improvement in the system is observed both for V and H polarizations, where the anomalous fluctuation apart from the sun peaks is fixed with the new cables.

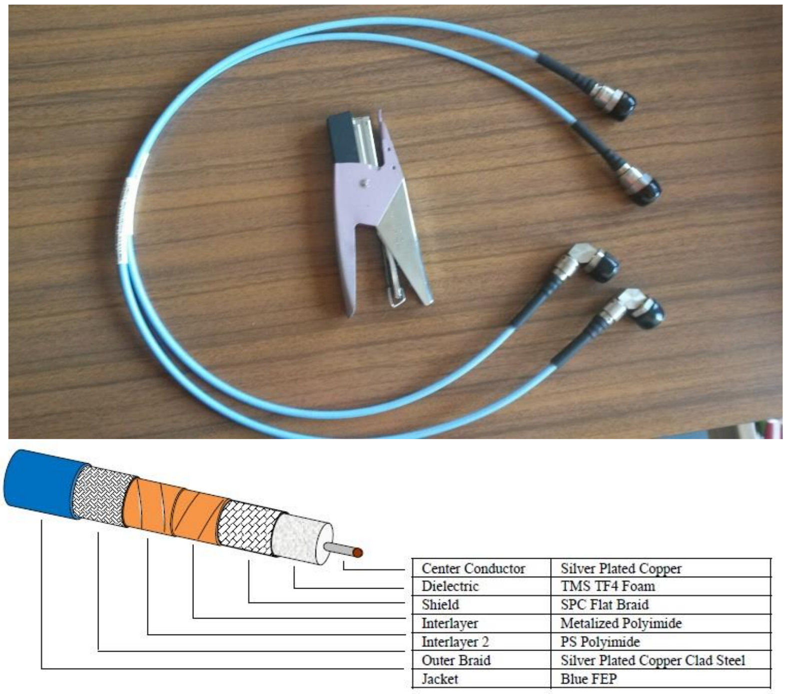

Figure 4-21: Photo of the new Phasetrack 210 cables (up) with the details of internal structure (down).

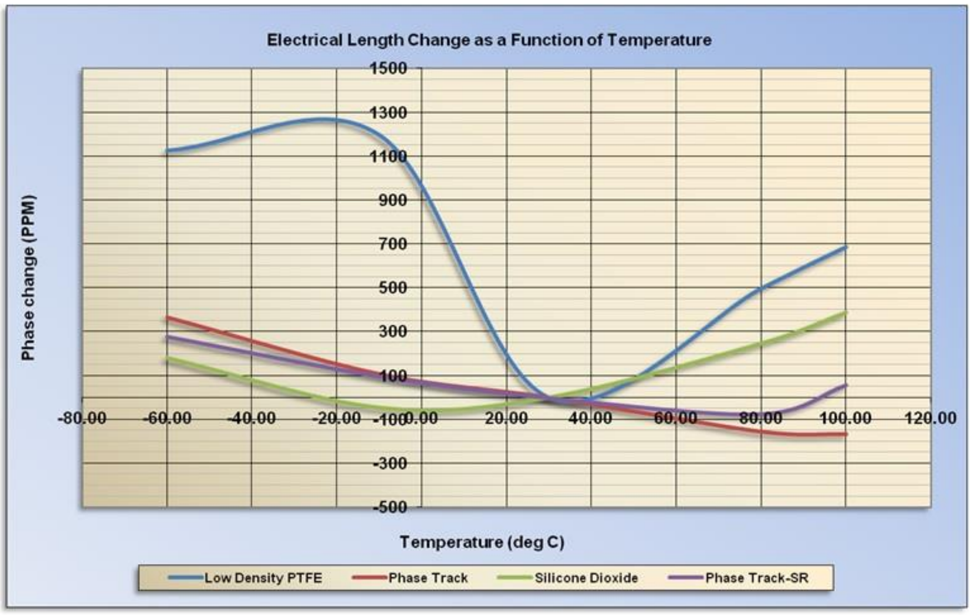

Figure 4-22: Phase characteristics as a function of temperature of the typical PTFE and the new Phasetrack cables. Data are from "Times Microwave Systems"

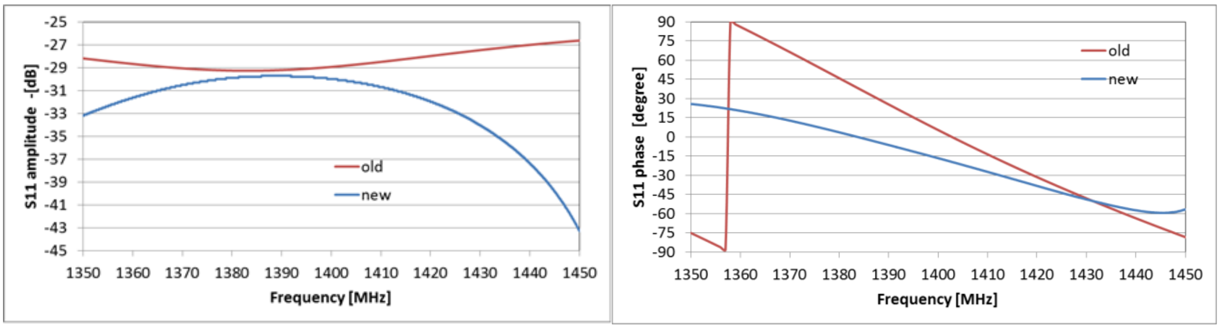

Figure 4-23: Amplitude (left) and phase characteristics (right) measured for the old PTFE and new Phasetrack 210 cables.

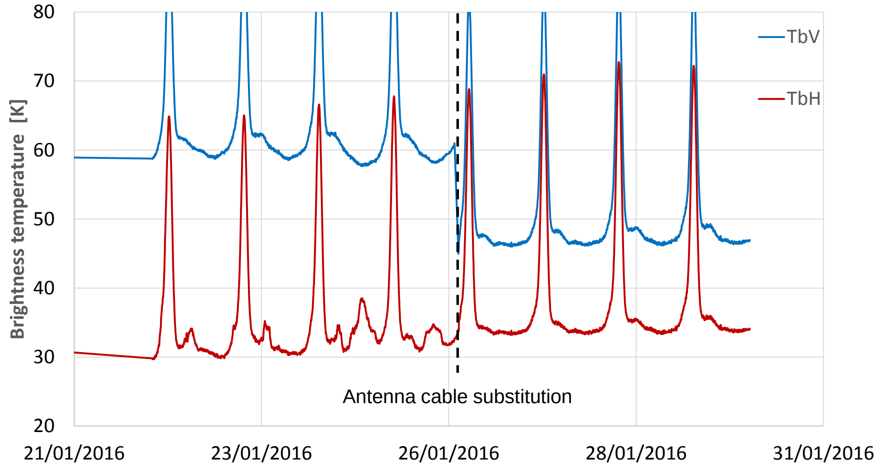

Figure 4-24: Brightness temperature before and after the cable substitution when observing clear sky.

4.3.2 Angular scan results

Angular observation were performed on Dec 2015 and June 2016 as reported in the acquisition Table 4-1. As already mentioned data are averaged every 5 samples (50 seconds) which means a shorter time than the standard acquisitions at 42 deg (3.33 minutes). This information is pointed out in [13]. The main reason is to better separate the transitional angles from the nominal ones in order to have a more precise characterization of each acquisition. Data are corrected for thermal variations with the procedure consolidated in section 4.2.2, then processed for absolute calibration.

The cumulative angular pattern which include both December and January acquisitions is shown in Figure 4-25 including the brightness temperature and standard deviations values for the range 30-120 degrees. Standard deviation (Figure 4-25) values are always lower than 0.3 for both polarization in the whole angular range, that is an indicator of a good thermal correction and calibration.

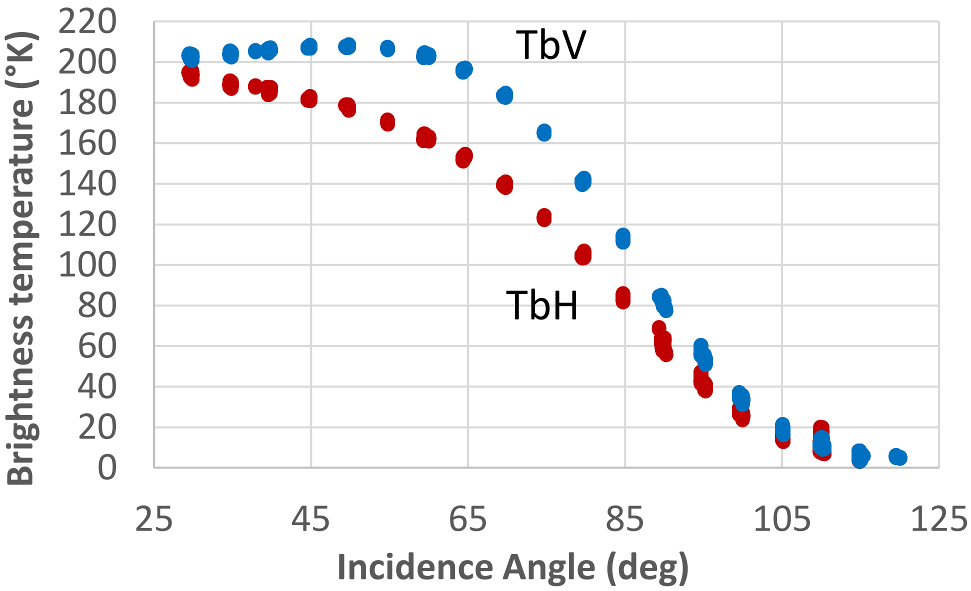

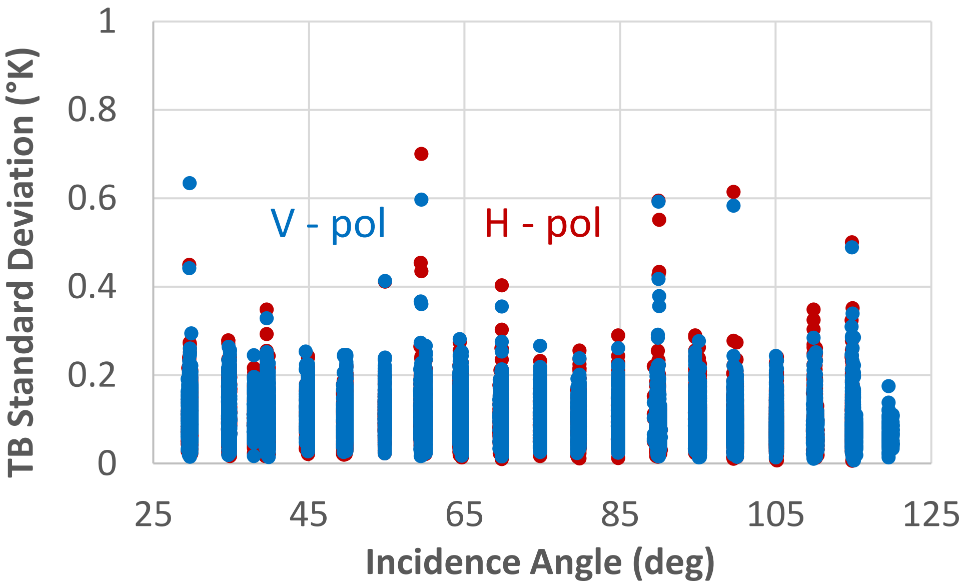

Figure 4-25: Angular pattern of calibrated TbV and TbH (up), and the standard deviations for each angle (down).

The angular values are cross checked with acquisitions from the other DomeX-3 campaigns, from 2013 to 2016, as in Figure 4-26. Figure shows a generally good agreement on the Tb values, especially at V- pol. while the H-pol is more variable, mostly depending on the modifications of snow layers.

The agreement is better pointed out in Figure 4-27, showing the annual deviation (2013-2016) from the multi-year average in the range 30 to 70 degrees. It can be observed that at V polarization the difference is on the order of ±1 K and doesn't change significantly as a function of incidence angle. The difference can be attributed both to natural Tb variability (annual fluctuation of the order of 1K are observed at V polarization) and absolute radiometer calibration. At H polarization 2016 data are slightly lower than the average (about 1k) but in this case it can be attributed to a small modification on snow surface properties.

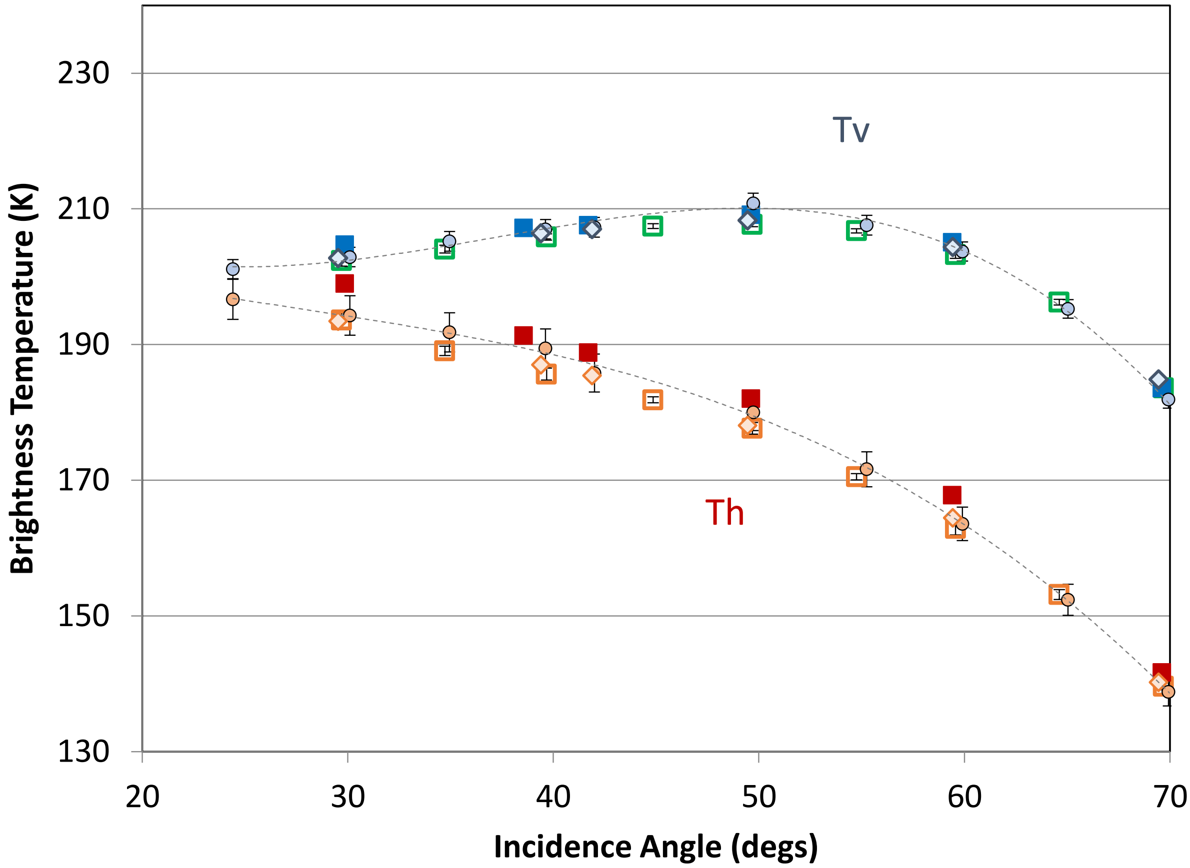

Figure 4-26: Brightness temperature as a function of the incidence angle at V- and H- pol covering observation from 2013 to 2016. V polarization: circle 2013 data, Diamond – 2014 data, blue square 2015 data, green square 2016 data. H polarization : circle 2013 data, Diamond – 2014 data, red square 2015 data, orange square 2016 data.

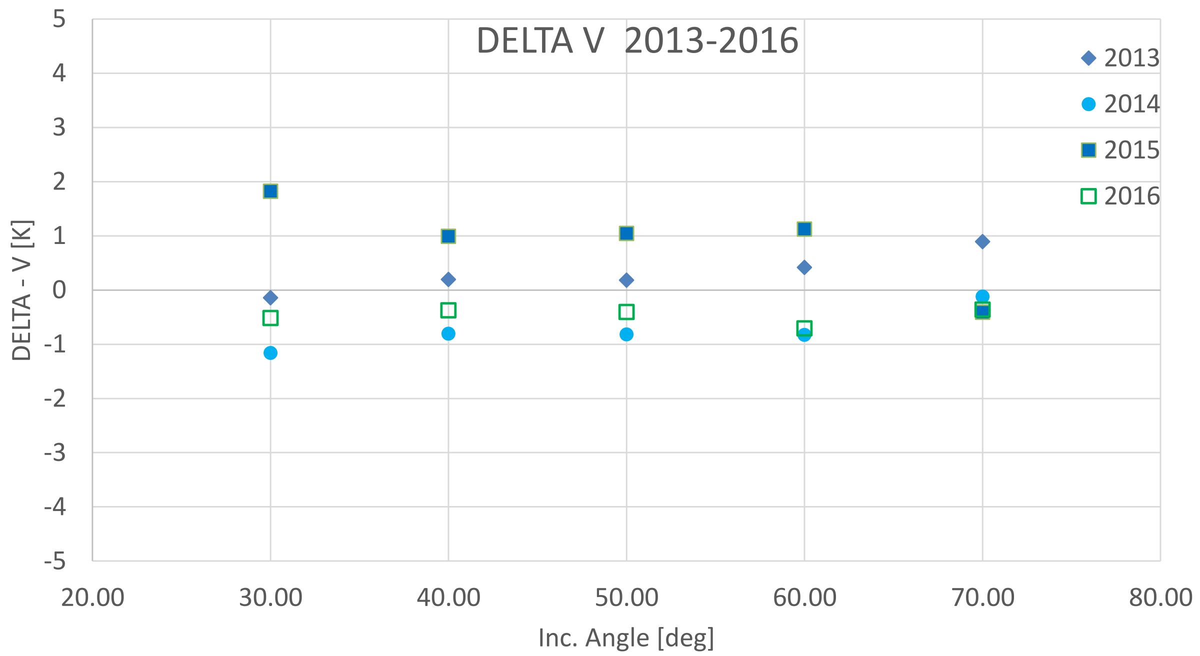

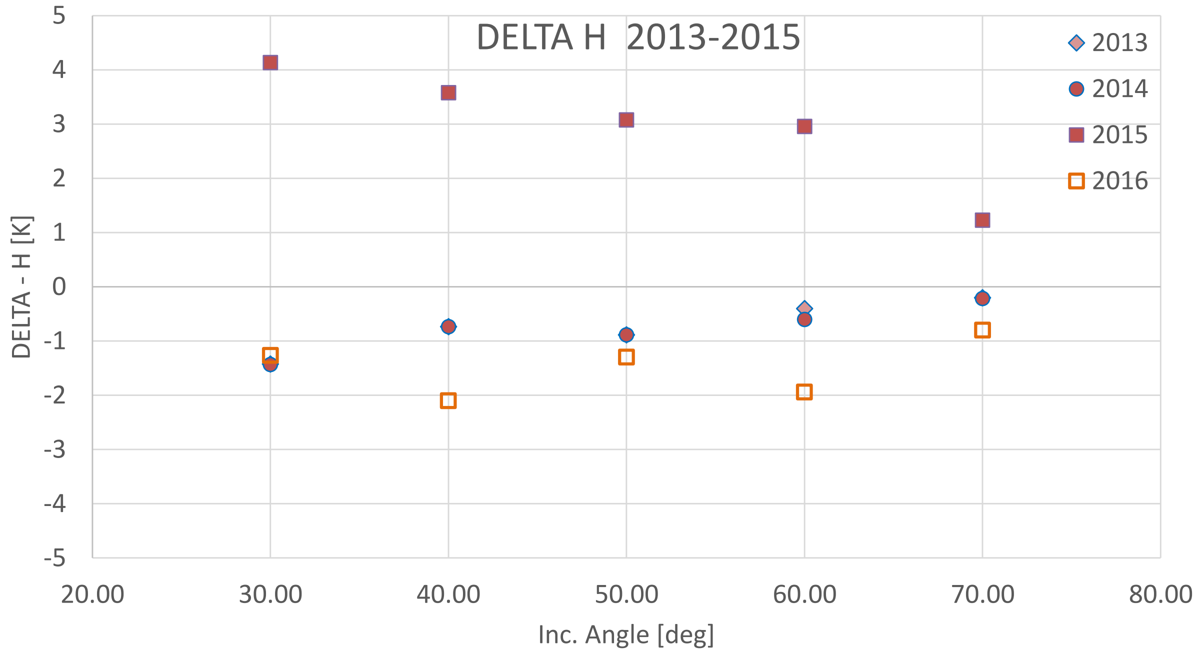

Figure 4-27: Difference variation between brightness temperature and the multi year average, from 2013 to 2016 for incidence angles between 30 and 70 degrees. (Top): V-pol and (Bottom) H- pol.

4.4 Comparison with SMOS data

Temporal series of calibrated/deconvoluted DomeX data acquired at 42 degrees are compared with SMOS L1C v620, in Figure 4-28. SMOS Tb are averaged over 9 pixels in the area around Concordia. Comparison show a good agreement between temporal trends for both V and H polarization while there are discrepancies for the absolute values. In details, the average value of DOMEX is 2.7K lower than SMOS at V-pol, and slightly higher at H-pol, 1.13 K as reported in Table 4-4. This values are in line with the comparison performed last year, pointed out in [7]. The differences are not yet explained, while we expect to be clarified after the improvement of absolute calibration and the antenna deconvolution that will be performed during the prosecution of the project. Data distribution has gaussian shape similar for both DOMEX and SMOS, while the standard deviation of DOMEX is lower (0.55K vs 1.37K at V- pol, 0.73K vs 2.07K at H-pol) as depicted in Figure 4-29.

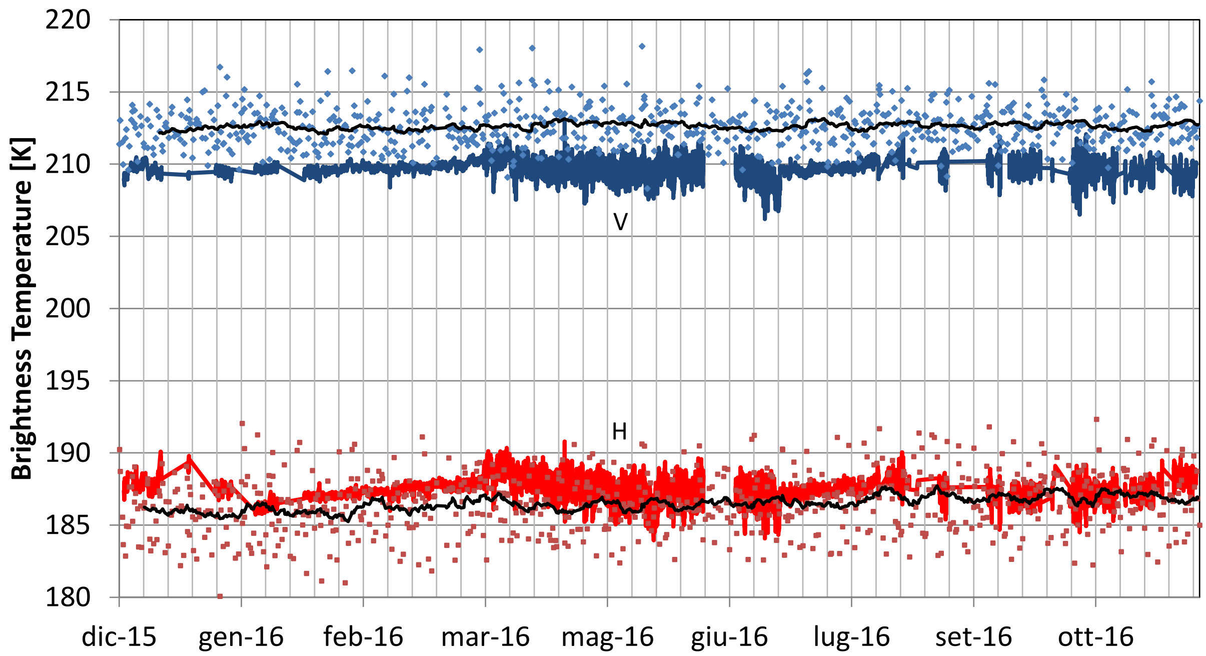

Figure 4-28: Comparison between DomeX data and SMOS v620. Blue and red markers identifies SMOS at V and H polarization respectively, while continuous black line is their moving average. Blue and red lines represent for DOMEX at V and H pol.

Table 4-4: Data statistics values for DOMEX and SMOS at 42 degrees for 2016 acquisitions.

	TBV (K)	St TBV (K)	TBH (K)	St TBH (K)
SMOS	212.37	1.37	186.3	2.07
DOMEX	209.67	0.55	187.43	0.73

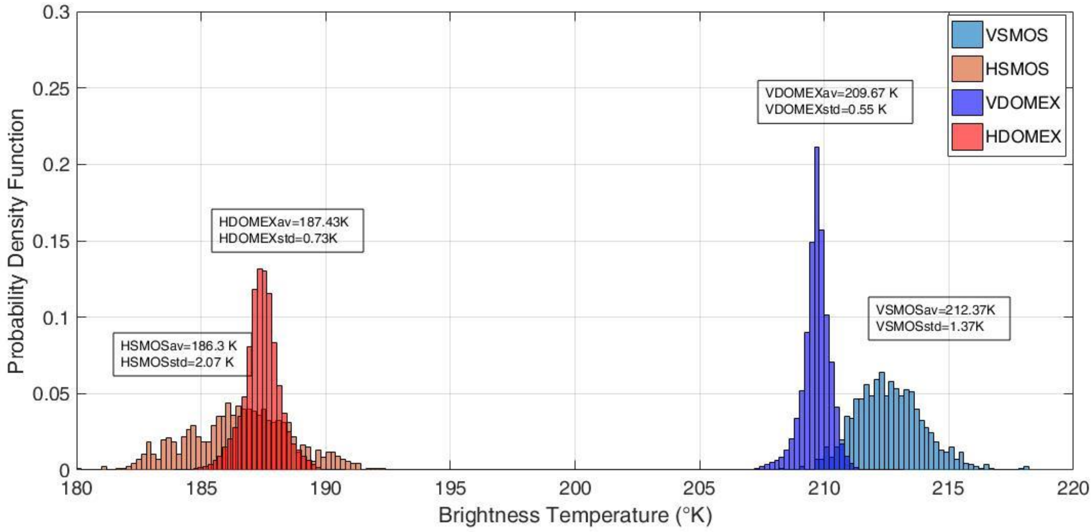

Figure 4-29: Normalized histograms of DOMEX data and SMOS, labelled with average and standard deviation values.

4.5 Snow Data

Snow temperature measurements at Dome C are carried out continuously since the Domex-1 campaign in 2004. At present the snow temperature is collected by means of a Datalogger and a string of PT100 probes in the same site since Domex-2 (2009-10 summer campaign). The data collected during Domex-3 project are summarized hereinafter.

4.5.1 Snow temperature

The snow temperature measurement is collected continuously at different depths by means of permanent PT100 probes located in close to the US tower. The nominal depth of the probes is the following: 5, 10, 25, 75, 100, 150, 200, 250, 300, 400, 500, 600, 800 and 1000 cm. These are the depth of the probes at the time of deployment. Actually, due to the snow accumulation, the probes get deeper as time passed and snow accumulates. Only the probes placed in the first meter (up to 150 cm) are realigned on every summer campaign at their nominal depth. Moreover, in the last summer campaign a probe was added and placed at 15 cm below surface. The annual series from 2015 to beginning of 2017 is shown in Figure 4-31, while the multi annual one from 2012 to 2016 showing the values at 10, 100, 300, 400, 500, 1000 cm below surface is in Figure 4-31. The variability at different depth is highlighted in Figure 4-32 where it is pretty clear that the surface probes are driven by the seasonal variability of temperature at the air/snow interface. The deeper probes are more stable and not affected by the air gradient. Values are shown in Table 4-5.

The IR temperature acquired in the same period is represented in Figure 4-30. A decreasing trend of the IR temperature of around 3K is observed in the data from 2012 to 2016, but this variability is surprisingly high and has to be explained with a more in depth analysis and compared with other IR sensors.

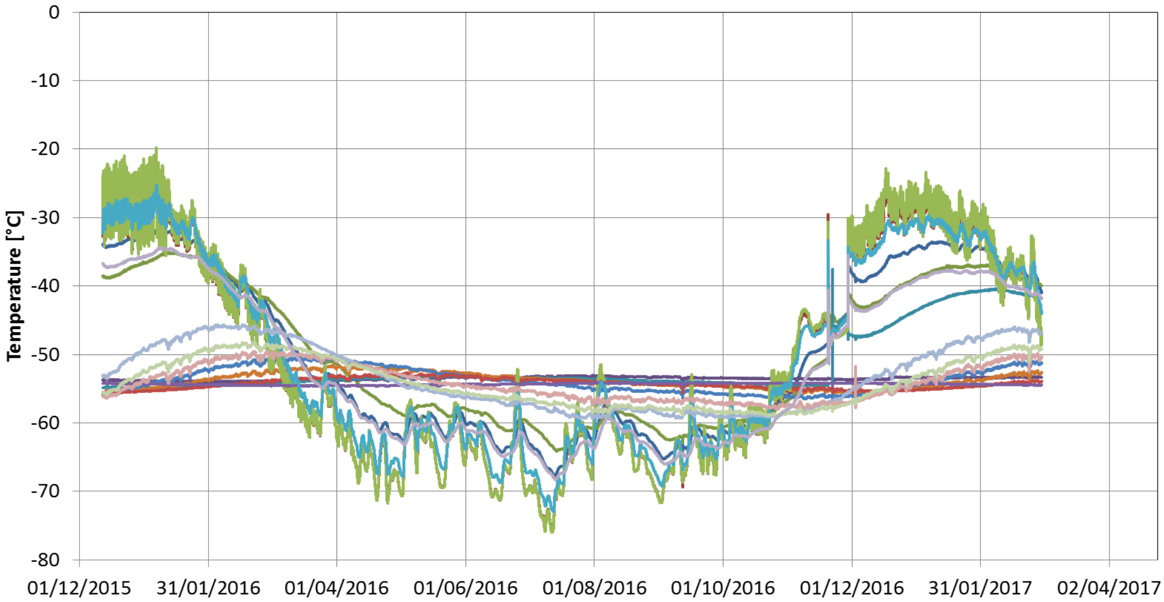

Figure 4-30: Snow temperature registered from 1/12/2015 to March 2017 at different depth (10 to 1000 cm)

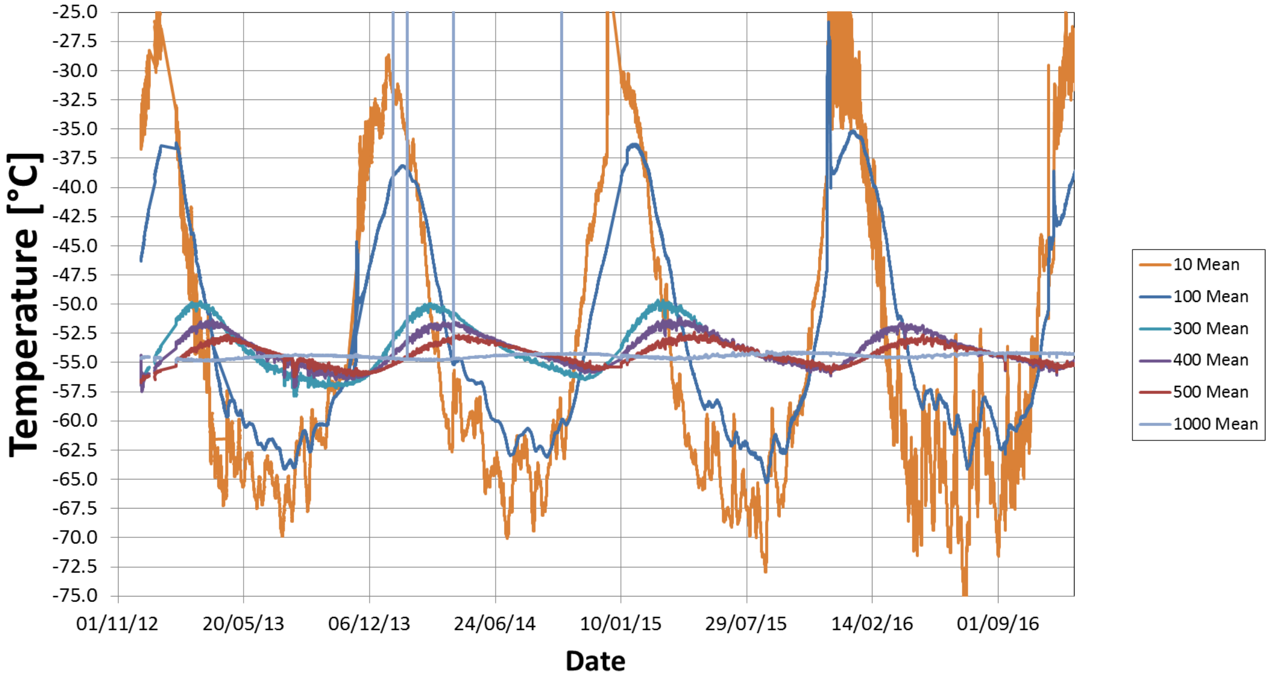

Figure 4-31: Snow Temperature measured at different depths since the beginning of DomeX-3 experiment.

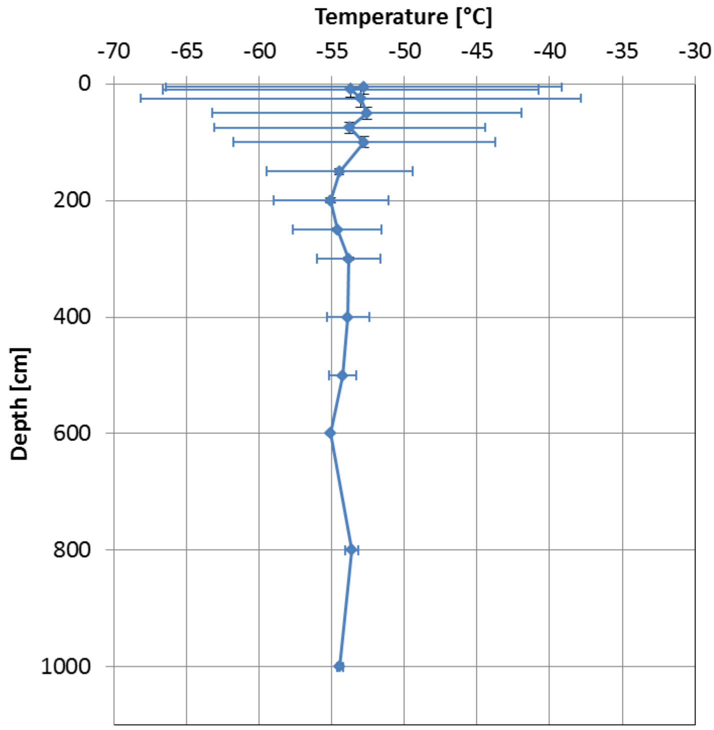

Figure 4-32: Variability of the snow temperature as a function of depth

Table 4-5: Average and Standard deviations value at different depths measured by the snow probes from 2012 to 2016.

Depth (cm)	Temp °C	Dev.s T °C
5	-52.8	13.62
10	-53.7	12.93
25	-53	15.17
50	-52.6	10.67
75	-53.8	9.34
100	-52.8	9.04
150	-54.5	5.03
200	-55.1	3.96
250	-54.6	3.06
300	-53.8	2.18
400	-53.9	1.44
500	-54.3	0.93
600	-55.1	0.7
800	-53.6	0.45
1000	-54.4	0.19

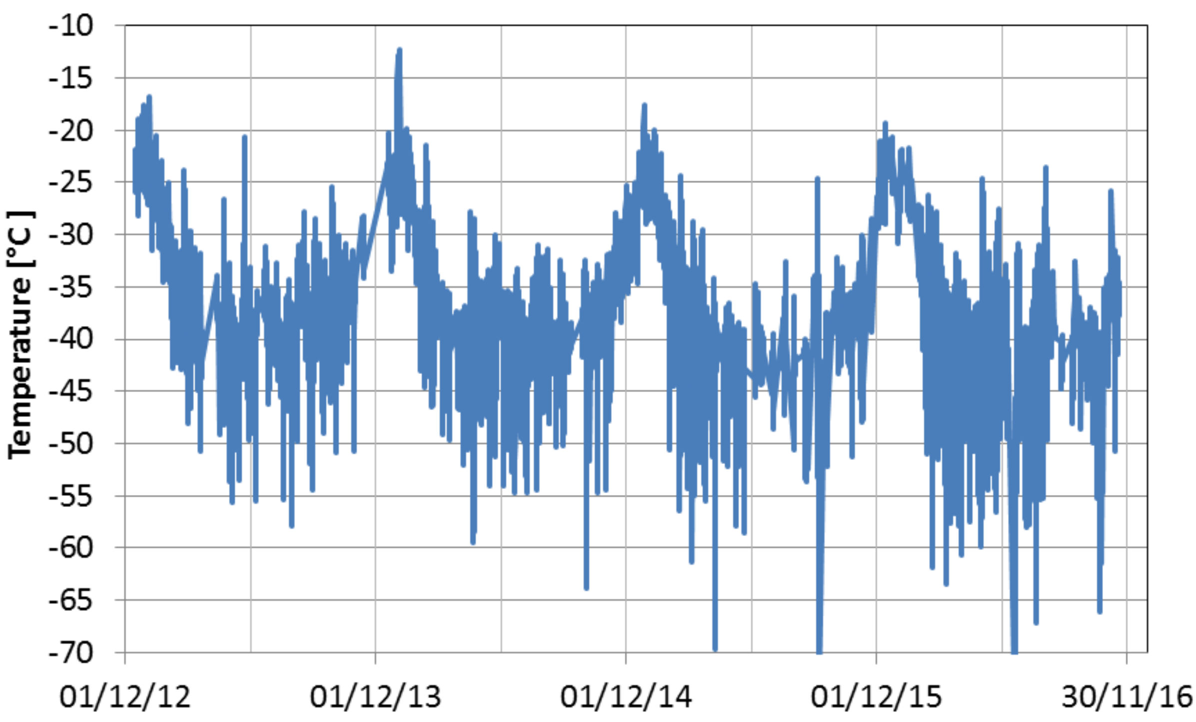

Figure 4-33: Infrared temperature from 2012 to end of 2016

5 DOMEX Publications

A list of paper published in 2016 related to DOMEX activity is contained here.

Macelloni, G., Leduc-Leballeur, M., Brogioni, M., Ritz, C., Picard, G. Analyzing and modeling the SMOS spatial variations in the East Antarctic Plateau (2016) Remote Sensing of Environment, 180, pp. 193-204.

Mecklenburg, S., Drusch, M., Kaleschke, L., Rodriguez-Fernandez, N., Reul, N., Kerr, Y., Font, J., Martin-Neira, M., Oliva, R., Daganzo-Eusebio, E., Grant, J.P., Sabia, R., Macelloni, G., Rautiainen, K., Fauste, J., de Rosnay, P., Munoz-Sabater, J., Verhoest, N., Lievens, H., Delwart, S., Crapolicchio, R., de la Fuente, A., Kornberg, M. ESA's Soil Moisture and Ocean Salinity mission: From science to operational applications (2016) Remote Sensing of Environment, 180, pp. 3-18.

Leduc-Leballeur, Marion; Picard, Ghislain ; Macelloni, Giovanni ; Brogioni, Marco ; Arnaud, Laurent ; Mialon, Arnaud ; Kerr, Yann H. L-band brightness temperature and snow surface properties at Dome C, Antarctica. ESA LIVING PLANET Symposium, Prague, 9-13 May 2016

Giovanni Macelloni, Francesco Montomoli, Marco Brogioni, On the Monitoring of the Antarctic Ice Sheet by L-band Space borne Radiometer, VIII Convegno Nazionale AIT, 22-23-24 giugno 2016, Palermo

Giovanni Macelloni, Marco Brogioni, Francesco Montomoli, Marion Leduc-Leballeur, Simulating the Antarctic plateau emission at L-band: effects of the different ice permittivity models, International Conference on Electromagnetic Wave Interaction with Water and Moist Substances May 23 - 27, 2016 Florence, Italy

Marion Leduc-Leballeur, Ghislain Picard, Giovanni Macelloni, Marco Brogioni, Laurent Arnaud, Arnaud Mialon, Yann H. Kerr, Modeling l-band brightness temperature in connection with snow surface properties variations at dome c, Antarctica. The 14th Specialist Meeting on Microwave Radiometry and Remote Sensing of the Environment (MicroRad 2016) will take place April 11-14, 2016, on Aalto University Campus, Espoo, Finland.

Macelloni, G., Leduc-Leballeur, M., Brogioni, M., Ritz, C., Picard, G. Modeling smos spatial variation in the east antarctic plateau , The 14th Specialist Meeting on Microwave Radiometry and Remote Sensing of the Environment (MicroRad 2016) will take place April 11-14, 2016, on Aalto University Campus, Espoo, Finland.

6 References

[1] ESA-contract Technical Support for the Deployment of an L-band Radiometer at Concordia Station, Final Report, 2005

[2] ESA Contract:20066/06/NL/EL 22046/08/NL/EL, - Technical Support for the Deployment of an L-band radiometer at Concordia Station during DOMEX-2- - Final Report . 2011

[3] Esa Contract: 4000105872/12/NL/NF - Technical Support for the Deployment of an L-band radiometer at Concordia Station during DOMEX-2 – Proposal –July 2012

[4] Esa Contract: 4000105872/12/NL/NF - Technical Support for the Deployment of an L-band radiometer at Concordia Station during DOMEX-2 – Campaign Implementation Plan, Deliverable D2 – October 2012

[5] Esa Contract: 4000105872/12/NL/NF - Technical Support for the Deployment of an L-band radiometer at Concordia Station during DOMEX-2 – Readiness Review Report, Deliverable D3 – October 2012

[6] ESA-ESTEC Contract 4000105872/12/NL/NF Technical Support for the Long-Term Deployment of an L-Band Radiometer at Concordia Station, First Year Report , D6, February 2014

[7] ESA-ESTEC Contract 4000105872/12/NL/NF Technical Support for the Long-Term Deployment of an L-Band Radiometer at Concordia Station, Second Year Report , D6, June 2016

[8] ESA Contract 18060/04/NL/CB - Technical Support for the Deployment of an L-band radiometer at Concordia Station Final Report . May 2006

[9] MODELING L-BAND BRIGHTNESS TEMPERATURE IN CONNECTION WITH SNOW SURFACE PROPERTIES VARIATIONS AT DOME C, ANTARCTICA. Marion Leduc-Leballeur, Ghislain Picard, Giovanni Macelloni, Marco Brogioni, Laurent Arnaud, Arnaud Mialon, Yann H. Kerr –Microrad 2016

[10] Fierz, C., Armstrong, R.L., Durand, Y., Etchevers, P., Greene, E., McClung, D.M., Nishimura, K., Satyawali, P.K., and Sokratov, S.A., 2009. The International Classification for Seasonal Snow on the Ground. IHP-VII Technical Documents in Hydrology N. 83, IACS Contribution N1, UNESCO-IHP, Paris.

[11] De Franceschi, G. Alfonsi L., Romano V, "ISACCO: an Italian project to monitor the high latitudes ionosphere by means of GPS receivers", GPS Solution, DOI 10.1007/s10291-006-0036-6, 2006

[12] S. Kristensen, S. Søbjærg, E. Balling, N. Skou DOME Cair CampaignEMIRAD Data. Presentation & Analysis Version 1.0 – August 2013 –ESA project report.

[13] ESTEC Contract 4000105872/12/NL/NF - Technical Support for the Long-Term Deployment of an L-band radiometer at Concordia Station, DATA DESCRIPTION: Instrument Status Report. March 2017.

[14] ANNEX 2 to CCN 6 to ESA Contract 4000105872/12/NL/FF/fk - Technical Support for the extension of the Long-Term Deployment of an L-Band Radiometer at Concordia Station (DOMEX-3 Extension), Statement of Work, 2016.

[15] Zirizzotti, A; Baskaradas, JA; Bianchi, C; Sciacca, U; Tabacco, IE; Zuccheretti, E; ,Glacio RADAR system and results,"Radar Conference, 2008. RADAR'08. IEEE",1-3,2008,IEEE

This page is intentionally left blank

TECHNICAL SUPPORT FOR THE LONG-TERM DEPLOYMENT OF AN L-BAND RADIOMETER AT CONCORDIA STATION

DATA DESCRIPTION: MW –IR TEMPERATURE

MAY 2017

EUROPEAN SPACE AGENCY STUDY CONTRACT REPORTS

ESTEC CONTRACT 4000105872/12/NL/NF

PREPARED BY

Giovanni Macelloni, Francesco Montomoli and Marco Brogioni

IFAC – CNR – SESTO FIORENTINO – ITALY

DATE: May 2017

This page is intentionally left blank

<table>
<tr><td colspan="4">ESA STUDY CONTRACT REPORT</td></tr>
<tr><td>EUROPEAN SPACE AGENCY STUDY CONTRACT REPORTS
ESTEC CONTRACT 4000105872/12/NL/NF</td><td colspan="2">TECHNICAL SUPPORT FOR THE LONG-TERM DEPLOYMENT OF AN L-BAND RADIOMETER AT CONCORDIA STATION</td><td>CONTRACTOR:
IFAC-CNR</td></tr>
<tr><td>ESA CR ( )NO:</td><td>STAR CODE:</td><td>No of volumes: 1
This is volume no: 1</td><td>CONTRACTOR'S REF:
MW-IR Temperature DataBase</td></tr>
<tr><td colspan="4">ABSTRACT:
This report contains the information of the MW-IR temperature data collected during DOMEX-3 experiment.</td></tr>
<tr><td colspan="4">The work described in this report was done under ESA Contract. Responsibility for the contents resides in the author or organisation that prepared it.</td></tr>
<tr><td colspan="4">AUTHORS: G. Macelloni, M. Brogioni, F.Montomoli (IFAC-CNR)</td></tr>
<tr><td colspan="2">ESA STUDY MANAGER:
T.Casal</td><td colspan="2">ESA BUDGET HEADING</td></tr>
</table>

This page is intentionally left blank

1 TITLE

1.1 Data set identification

DOMEX-3 Microwave and Infrared Radiometers data.

1.2 Revision date of this document (dd/mm/yyyy)

29/05/2017

1.3 INVESTIGATOR(S)

Dr. Giovanni Macelloni
Earth Observation Department
Istituto di Fisica Applicata (IFAC)
Consiglio Nazionale delle Ricerche
Via Madonna del piano 10 - 50019 -Sesto Fiorentino (Fi) - Italy
Tel. + 39 055 5226495 – Fax + 39 055 5226467
E-mail: G.Macelloni@ifac.cnr.it

2 EQUIPMENT

2.1 Instrument description.

The measurements were carried out with IFAC microwave radiometer called RADOMEX, please refers to the Year report 2016 of the project for more information.

2.2 Platform (Satellite, Aircraft, Ground).

Ground

2.3 Key variables.

Microwave brightness temperature at 1.4 GHz (L-band), horizontal and vertical polarization, Infrared temperature (8-14 μm).

2.4 Instrument measurement geometry.

Data were collected from the tower-mounted radiometer from December 2015 to November 2016 at different incidence angles within the 30° - 120° range with respect to nadir (i.e 0° = nadir view) in the North-West direction. Different procedure have been followed for the acquisition as described in the Final Report and in the Experiment Support Plan of the project.

2.5 Manufacturer of instrument.

Instruments were designed and developed at IFAC CNR Firenze Italy

2.6 Calibration.

Calibration procedure was described in DOMEX-2 –Final report.

3 PROCEDURE

3.1 Data acquisition methods.

Data were collected automatically from the tower-mounted radiometer 24 hours/day. Data acquisition and platform movement were automatically controlled by means of a PC placed in the box; and the experiment was monitored remotely using a Local Area Network connection.

The following parameters were used for the acquisitions:
Integration time (measurement and calibration): 4 second
Number of measurements between calibration: 8 (4 H and 4 V)
Measurement Time (for each position): variable

IMPORTANT NOTE : In the dataset is represented the number of measurements, Tb mean value and standard deviation collected at each single position.

3.2 Spatial characteristics.

3.2.1 Spatial coverage.

Data were acquired at a fixed position at:

Coordinates: 75.0989°S 123.3005°E

Altitude: 3250 M

The antenna foot-print (HPBW) ranged from 10x14 m^2 at θ = 20° to 10 x 160 m^2 at θ = 70° .

3.2.2 Spatial resolution.

Please refers to Experiment Implementation Plan

3.2.3 Temporal characteristics.

Please refers to Experiment Implementation Plan

3.2.4 Temporal coverage.

Data represented in this dataset were acquired from December 2015 to November 2016

4 DATA DESCRIPTION

4.1 Table definition with comments.

The data base is contained in the file DOMEX_3_FOURTHYEAR_2016_MWDATA.txt in ASCII format.

It could be easily opened with MS Excel or Matlab.

The files are composed by a table of 121309 Rows + 1 (header) and 37 Columns

Column description:

c1 = Date – time DD/MM/YY hh:mm
c2 = Number of samples
c3 = Sun zenith position (degs)
c4 = Sun angular position (degs)

c5 = Quality flag; 0 = quality check passed; 1 = quality check not passed only for V-pol; 2 = quality check not passed only for H-pol; 3 = quality check not passed
c6 = sun flag; 0 = sun not in front of the antenna; 1 = sun in the antenna pattern
c7 = calibration scheme; 1 = frequent calibration hot and cold load; 2 = frequent calibration fixed gain, cold load; 3 = frequent calibration cold load and noise source.
c8 = TVL= Brightness Temperature L band – Vertical polarization (K)
c9 = Stdev TVL= Standard deviation of #c8 (K)
c10 = THL= Brightness Temperature L band – Horizontal polarization (K)
c11 = Stdev THL= Standard deviation of #c10 (K)
c12 = Theta = Incidence Angle (degrees)
c13 = SdevTheta = Standard deviation of #c12 (degs)
c14 = Theta = Azimuth Angle (degrees)
c15 = SdevTheta = Standard deviation of #c14 (degs)
c16 = Tir= Temperature of the calibrator of IR sensor (°C)
c17 = Stdev Tir= Standard deviation of #c16 (°C)
c18 = Temperature of Tns internal to the Radiometer receiver
c19 = Stdev Tns= Standard deviation of #c18 (°C)
c20 = Temperature of Tsw internal to the Radiometer receiver
c21 = Stdev Tsw= Standard deviation of #c20 (°C)
c22 = Temperature of Tcables1 internal to the Radiometer receiver
c23 = Stdev Tcables= Standard deviation of #c22 (°C)
c24 = Temperature of Tcables2 internal to the Radiometer receiver
c25 = Stdev Tcables= Standard deviation of #c24 (°C)
c26 = Temperature of T_H_omt connector
c27 = Stdev T_H_omt= Standard deviation of #c26 (°C)
c28 = Temperature of T_V_omt connector
c29 = Stdev T_V_omt= Standard deviation of #c28 (°C)
c30 = Temperature of T_H_rad connector
c31 = Stdev T_H_omt= Standard deviation of #c30 (°C)
c32 = Temperature of T_V_rad connector
c33 = Stdev T_V_rad= Standard deviation of #c32 (°C)
c34 = Temperature of T_OMT
c35 = Stdev T_ant= Standard deviation of #c34 (°C)
c36 = Temperature of Antenna front part
c37 = Stdev T_ant= Standard deviation of #c36 (°C)

- Missing data are identified as NaN

5 DATA QUALITY

5.1 Data Manipulations

As described in detail in the DOMEX Final Report the data at L band were processed and calibrated.

5.2 Sources of error.

The errors in the measurement were mainly related to the data post-processing. The adopted procedure is described in the Final Report of the project.

5.3 Quality assessment.

The minimum detectable temperature variation of the radiometer (sensitivity) was 0.3 K (with τ = 2 sec), and the accuracy (repeatability) was better than 0.5 K over a period of 30 days.

5.4 Quality flag definition.

The quality flag (column # c5 of the file) is defined as follows:
0 - Tb standard deviation computed over number of samples defined in column # c2 at V and H pol. Is lower than 1 K
1 - Tb standard deviation computed over number of samples defined in column # c2 at V pol. Is higher than 1 K
2 - Tb standard deviation computed over number of samples defined in column # c2 at H pol. Is higher than 1 K
3 - Tb standard deviation computed over number of samples defined in column # c2 at V and H pol. Is higher than 1 K.

A value higher than 0 imply a degradation of the measure.

6 REFERENCES

Technical Support for the Long-Term Deployment of an L-Band Radiometer at Concordia Station
Yearly Report – Third Year Report, June 2016 EUROPEAN SPACE AGENCY STUDY
ESTEC Contract 4000105872/12/NL/NF –Macelloni et. Al

7 DATA POLICY

The participants (IFAC and CVA) have the exclusive right of access to and exploitation of data lather than 6 months after the end of the project (presentation of the final report). After this date dissemination of the dataset will be performed by ESA under the control and with the approval of IFAC.

TECHNICAL SUPPORT FOR THE LONG-TERM DEPLOYMENT OF AN L-BAND RADIOMETER AT CONCORDIA STATION

DATA DESCRIPTION: SNOWTEMPERATURE

MAY 2017

EUROPEAN SPACE AGENCY STUDY CONTRACT REPORTS

ESTEC CONTRACT 4000105872/12/NL/NF

PREPARED BY

Giovanni Macelloni, Simone Pettinato, Francesco Montomoli and Marco Brogioni

IFAC – CNR – SESTO FIORENTINO – ITALY

DATE: May 2017

This page is intentionally left blank

<table>
<tr><td colspan="4">ESA STUDY CONTRACT REPORT</td></tr>
<tr><td>EUROPEAN SPACE AGENCY STUDY CONTRACT REPORTS
ESTEC CONTRACT 4000105872/12/NL/NF</td><td colspan="2">TECHNICAL SUPPORT FOR THE LONG-TERM DEPLOYMENT OF AN L-BAND RADIOMETER AT CONCORDIA STATION</td><td>CONTRACTOR:
IFAC-CNR</td></tr>
<tr><td>ESA CR ( )NO:</td><td>STAR CODE:</td><td>No of volumes: 1
This is volume no: 1</td><td>CONTRACTOR'S REF:
Snow Temperature DataBase</td></tr>
<tr><td colspan="4">ABSTRACT:
This report contains the information of the snow temperature data collected during DOMEX-3 experiment.</td></tr>
<tr><td colspan="4">The work described in this report was done under ESA Contract. Responsibility for the contents resides in the author or organisation that prepared it.</td></tr>
<tr><td colspan="4">AUTHORS: G. Macelloni, M. Brogioni, F.Montomoli (IFAC-CNR)</td></tr>
<tr><td colspan="2">ESA STUDY MANAGER:
T.Casal</td><td colspan="2">ESA BUDGET HEADING</td></tr>
</table>

This page is intentionally left blank

1 TITLE

1.1 Data set identification

DOMEX-3 Snow Temperature Data

1.2 Revision date of this document (yyyy/mm/dd)

2017/05/29

2 INVESTIGATOR(S)

Dr. Giovanni Macelloni
Earth Observation Department
Istituto di Fisica Applicata (IFAC)
Consiglio Nazionale delle Ricerche
Via Madonna del piano 10 - 50019 -Sesto Fiorentino (Fi) - Italy
Tel. + 39 055 5226495 – Fax + 39 055 5226467
E-mail: G.Macelloni@ifac.cnr.it

3 EQUIPMENT

3.1 Instrument description.

The measurements were carried out with LSI LASTEM –data logger. –Model EL 305 and EL 105, Probes: PT100 Din-A
Please refers to http://www.lsi-lastem.it for more information.

3.2 Platform (Satellite, Aircraft, Ground).

Ground

3.3 Key variables.

Snow Temperature measured at different depth (range 0-10 m)

3.4 Instrument measurement geometry.

The temperature profile of the first 10 m of the snow pack was measured by using 10 probes. The probes (PT100 –DIN-A) were placed at different depths as described Table 1

Table 1

Probe N	Depth (cm)
1	5
2	10
3	25
4	50
5	75
6	100
7	150
8	200
9	250
10	300
11	400
12	500
13	600
14	800
15	1000
16	AIR

3.5 Manufacturer of instrument.

Instruments were designed and developed by LSI-LASTEM (Italy).

4 PROCEDURE

4.1 Data acquisition methods.

Data were collected automatically by the data logger.

Data were acquired at each minute and recorded at each hour (mean, maximum, minimum).

IMPORTANT NOTE : In the dataset is represented the mean value are represented, the typical value of the standard deviation is less than 0.05 °C, maximum value is 0.1 °C

4.2 Spatial characteristics.

Spatial coverage.

Data were acquired at a fixed position at,:

Coordinates: 75.0989°S, 123.3005°E.
Altitude: 3250 m

Please refers to the Final Report of the project for more information

4.3 Temporal characteristics.

Temporal coverage.
Data represented in this dataset were acquired from January 1, 2016 to December 31, 2015.

5 5. DATA DESCRIPTION

Snow temperature probe collected at 600 cm was damaged after 23/11/2016. A new probe was placed to measure the air temperature at 50 cm above surface, on 5/12/2016.

5.1 Table definition with comments.

The data base is contained in the file **DOMEX3_snowtemp_database3.txt** as ASCII format.

It could be easily opened with MS Excel or Matlab.

The file is composed by a table 9264 rows + 1 (header) and 49 Columns.

Columns description:
c1 =Date – time YYYYMMDDTHHMMSS
c2 = T1= Minimum Temperature Probe 1 (50 cm) (°C)
c3 = T1= Mean Temperature Probe 1 (50 cm) (°C)
c4 = T1= Maximum Temperature Probe 1 (50 cm) (°C)
c5 = T2= Minimum Temperature Probe 1 (10 cm) (°C)
c6 = T2= Mean Temperature Probe 1 (10 cm) (°C)

c7 = T2= Maximum Temperature Probe 1 (10 cm) (°C)
c8 = T3= Minimum Temperature Probe 1 (100 cm) (°C)
c9 = T3= Mean Temperature Probe 1 (100 cm) (°C)
c10 = T3= Maximum Temperature Probe 1 (100 cm) (°C)
c11 = T4= Minimum Temperature Probe 1 (800 cm) (°C)
c12 = T4= Mean Temperature Probe 1 (800 cm) (°C)
c13 = T4= Maximum Temperature Probe 1 (800 cm) (°C)
c14 = T5= Minimum Temperature Probe 1 (600 cm) (°C)
c15 = T5= Mean Temperature Probe 1 (600 cm) (°C)
c16 = T5= Maximum Temperature Probe 1 (600 cm) (°C)
c17 = T6= Minimum Temperature Probe 1 (400 cm) (°C)
c18 = T6= Mean Temperature Probe 1 (400 cm) (°C)
c19 = T6= Maximum Temperature Probe 1 (400 cm) (°C)
c20 = T7= Minimum Temperature Probe 1 (300 cm) (°C)
c21 = T7= Mean Temperature Probe 1 (300 cm) (°C)
c22 = T7= Maximum Temperature Probe 1 (300 cm) (°C)
c23 = T8= Minimum Temperature Probe 1 (500 cm) (°C)
c24 = T8= Mean Temperature Probe 1 (500 cm) (°C)
c25 = T8= Maximum Temperature Probe 1 (500 cm) (°C)
c26 = T9= Minimum Temperature Probe 1 (5 cm) (°C)
c27 = T9= Mean Temperature Probe 1 (5 cm) (°C)
c28 = T9= Maximum Temperature Probe 1 (5 cm) (°C)
c29 = T10= Minimum Temperature Probe 1 (1000 cm) (°C)
c30 = T10= Mean Temperature Probe 1 (1000 cm) (°C)
c31 = T10= Maximum Temperature Probe 1 (1000 cm) (°C)
c32 = T11= Minimum Temperature Probe 1 (25 cm) (°C)
c33 = T11= Mean Temperature Probe 1 (25 cm) (°C)
c34 = T11= Maximum Temperature Probe 1 (25 cm) (°C)
c35 = T12= Minimum Temperature Probe 1 (AIR) (°C)
c36 = T12= Mean Temperature Probe 1 (AIR) (°C)
c37 = T12= Maximum Temperature Probe 1 (AIR) (°C)
c38 = T13= Minimum Temperature Probe 1 (150 cm) (°C)
c39 = T13= Mean Temperature Probe 1 (150 cm) (°C)
c40 = T13= Maximum Temperature Probe 1 (150 cm) (°C)
c41 = T14= Minimum Temperature Probe 1 (250 cm) (°C)
c42 = T14= Mean Temperature Probe 1 (250 cm) (°C)
c43 = T14= Maximum Temperature Probe 1 (250 cm) (°C)
c44 = T15= Minimum Temperature Probe 1 (200 cm) (°C)
c45 = T15= Mean Temperature Probe 1 (200 cm) (°C)
c46 = T15= Maximum Temperature Probe 1 (200 cm) (°C)
c47 = T16= Minimum Temperature Probe 1 (75 cm) (°C)
c48 = T16= Mean Temperature Probe 1 (75 cm) (°C)

c49 = T16= Maximum Temperature Probe 1 (75 cm) (°C)

- Missing data are identified as NaN

6 *DATA QUALITY*

6.1 Data Manipulations

Data were not manipulated

7 Sources of error.

Please refers to LSI-Lastem information

8 Quality assessment.

Please refers to LSI-Lastem information

9 REFERENCES

[1] LSI-LASTEM user manual (http://www.lsi-lastem.it/pdf/instum00031.pdf)

[2] TECHNICAL SUPPORT FOR THE LONG-TERM DEPLOYMENT OF AN L-BAND RADIOMETER AT CONCORDIA STATION

10 DATA POLICY

The participants (IFAC and CVA) have the exclusive right of access to and exploitation of data lather than 6 months after the end of the project (presentation of the final report). After this date dissemination of the dataset will be performed by ESA under the control and with the approval of IFAC.